Received: 6 January 2022 | Revised: 10 May 2022 | Accepted: 31 May 2022 | Published on: 6 September 2022

DOI: 10.1002/num.22906

RESEARCH ARTICLE

WILEY

Towards hybrid two-phase modelling using linear domain decomposition

David Seus[1] | **Florin A. Radu**[2] | **Christian Rohde**[1]

[1]Institute of Applied Analysis and Numerical Simulation, University of Stuttgart, Stuttgart, Germany
[2]Department of Mathematics, University of Bergen, Bergen, Norway

Correspondence
David Seus, Institute of Applied Analysis and Numerical Simulation, University of Stuttgart, Pfaffenwaldring 57, 70569 Stuttgart, Germany.
Email: david.seus@ians.uni-stuttgart.de

Funding information
University of Bergen (UIB); E.ON Stipendienfonds, Grant/Award Number: T0087/30890/17; Research Foundation (DFG), Grant/Award Number: 327154368–SFB-1313.

Abstract

The viscous flow of two immiscible fluids in a porous medium on the Darcy scale is governed by a system of nonlinear parabolic equations. If infinite mobility of one phase can be assumed (e.g., in soil layers in contact with the atmosphere) the system can be substituted by the scalar Richards model. Thus, the porous medium domain may be partitioned into disjoint subdomains where either the full two-phase or the simplified Richards model dynamics are valid. Extending the previously considered one-model situations we suggest coupling conditions for this hybrid model approach. Based on an Euler implicit discretization, a linear iterative (L-type) domain decomposition scheme is proposed, and proved to be convergent. The theoretical findings are verified by a comparative numerical study that in particular confirms the efficiency of the hybrid ansatz as compared to full two-phase model computations.

KEYWORDS

domain decomposition, hybrid modeling, LDD scheme, Richards equation, two-phase flow in porous media

1 | INTRODUCTION

Multiphase flow through porous media occurs for a wide variety of natural and technical processes. Examples in soil-related environmental sciences comprise enhanced oil recovery, remediation of contaminated soils, CO_2 and energy storage systems or evaporation processes in the vadose zone. In the technological realm we mention the design of filters, fuel cells or damping materials. Mathematical modeling and numerical simulation are essential tools for the understanding of multiphase flow processes. However, due to varying material properties or changing flow regimes the governing equations can become strongly heterogeneous leading to severe mathematical and in particular computational problems. To meet these challenges, domain decomposition methods are an established approach (see e.g., [3]). The basic idea is to split the domain in subdomains such that each of these subdomains can be equipped with their respective model and numerical solver. Following an iterative scheme and by construction of analytically and numerically appropriate coupling conditions an approximate solution on the original mono-domain can then be recovered.

In contrast to existing approaches for homogeneous two-phase flow models, the purpose of the present contribution is the development and analysis of a nonoverlapping domain decomposition method for *hybrid* modeling. We consider Darcy scale flow of two incompressible, viscous and immiscible fluids in porous media. Let the fluids be denoted as the wetting (w) and the nonwetting (nw) phase, respectively. The computational domain is decomposed into subdomains with the flow either governed by the full two-phase (TP) model or by the *simpler* Richards (R) model. The latter applies for example, for high mobilities of the nonwetting phase. Such regimes occur typically in the upper layers of unconfined aquifers that are in contact with the atmosphere but fail to be valid in deeper regions of the vadose zone. The partition might come along with changes in the relative permeability functions, fluid viscosities and densities, as well as in porosities and intrinsic permeabilities. The major advantage of the hybrid approach is the possible gain of computing time that can be obtained when substituting the full two-phase model system by the (scalar) Richards equation on parts of the domain.

First, in Section 2, we present coupling conditions for the hybrid two-phase– Richards (TP–R) model across the interfaces of subdomains. In fact, the coupling condition for the nonwetting flux in the two-phase model is not at all obvious, given that on the Richards model domain there is no equation for the nonwetting phase. This leads to an unmatched number of unknowns on the different subdomains. We therefore introduce two different coupling conditions depending on the (non)occurrence of gravitational forces. Extending our approach for homogeneous two-phase flow models in [1, 2], we proceed then with the time-discrete problem and introduce a domain decomposition solver based on simultaneous L-scheme linearization, see [4, 5]. The resulting scheme is called LDD-TP–R solver. We further provide a consistency result that ensures that (in case of convergence) the LDD-TP–R solver provides the mono-domain solution (Lemma 1). Section 3 contains the core analytical result of the paper, that is the convergence of the LDD-TP–R solver in Theorem 1. The idea of the proof is based on bounding the series of iteration errors which implies that the sequence of iteration errors must vanish. A key ingredient to achieve this is to detect matching interface Robin-type terms such that telescopic sums are obtained. In fact, the latter is only possible if the pressure traces that are part of the Robin-type coupling condition on interfaces act as functionals via the $H^{1/2}_{00}(\Gamma)$-scalar product and not in the classical way via the dual pairing $H^{-1/2}(\Gamma) \times H^{1/2}_{00}(\Gamma)$ that stems from the L^2-scalar product, compare Remark 2 as well as [6]. The convergence is guaranteed under a restriction on the time-step size which reduces to the restrictions obtained in [1, 2] for the respective single-model cases.

To limit the notational overhead and to keep the focus, Sections 2 and 3 are restricted to a two-domain partition. In Section 4 we generalize the LDD-TP–R solver to a multidomain situation. Finally, Section 5 provides the numerical validation of the performance of the LDD-TP–R solver. Illustrative simulations on two- and multidomain partitions for realistic soil parameters are performed. The numerical results confirm the convergence statement from Theorem 1 revealing linear rates. We further perform a sensitivity analysis on numerical and solver parameters (mesh size, time step, Robin parameters, L-scheme parameters). For the multidomain case, a special focus is set on gravity effects. Most importantly we show the advantage of the hybrid model approach in terms of computational efficiency, as compared to the use of the full two-phase flow model on the entire mono-domain. The paper ends with an outlook how the LDD-TP–R solver can be utilized for an error-controlled model-adaptive approach.

We conclude this introduction with a short overview on the literature for related domain-decomposition methods and solvers for multiphase flow in porous media.

Independently of the underlying numerical approaches, domain decomposition methods allow to reduce the computational complexity of the problem, and to follow parallel solver techniques. We refer to [7, 8] for general descriptions of the field. Optimizing the parameters in the transmission conditions is an important issue in all domain decomposition methods, see for example, [9] and references therein. Concerning porous media flow on the Darcy scale, we refer to [10] for an overview of different overlapping domain decomposition strategies. A combined non-overlapping domain decomposition method and multigrid solver approach for the Richards equation has been presented in [11]. In [12, 13] algorithms for multiphase porous media flow are introduced, including a-posteriori estimates to optimize the parameters and the number of iterations. A time-adaptive domain decomposition concept is pursued in [14]. Convergence of a Schwarz waveform relaxation method is established in [15] for the transport equation in the fractional flow formulation of two-phase flow. Lunowa et al. in [16] apply ideas from [1, 2] to a dynamic capillary pressure model with hysteresis on a two-domain setting. The work [17] is concerned with two-phase flow with discontinuous capillary pressures. None of these works address the case of a hybrid model ansatz.

In this work, we combine the domain-decomposition method for each time step with an L-scheme (see [4, 5]) to linearize the complete system. This linearization approach, which is a stabilized Picard method has been used for a variety of applications, for example, nonlinear poromechanics [18] or fully coupled flow and transport [19]. The L-scheme has the advantage of not involving the computation of derivatives, in contrast to the Newton or the modified Picard method [20]. Moreover, its implementation is very easy, it is globally convergent and the linear problems that need to be solved within each iteration are much better conditioned as the ones stemming from e.g. the Newton method, see [5]. Nevertheless, a drawback of L-schemes is their slower (linear) convergence in comparison to Newton's scheme. Albeit faster converging L-schemes have been suggested in [5, 21], this article adheres to the standard L-scheme, focusing on an LDD scheme for a flexible, subdomain-wise combination of the Richards equation and the full two-phase flow model. The decoupling of the subproblems resulting from the domain decomposition in the formulation of the L-scheme presented here is achieved through a Robin-type interface term involving a parameter. It is well known for linear problems (both elliptic and parabolic) that the convergence rate depends on the choice of this parameter and that optimal choices are possible. While we do not dwell on such questions in this work, we point the reader interested in such aspects to the works [22, 23, 24], and [25] as well as references therein.

2 | TWO-PHASE FLOW MODELS AND THE LDD-TP–R SOLVER FOR THE TWO-DOMAIN CASE

In this section, we introduce the notations, present the mathematical models (two-phase flow, the Richards equation and the hybrid model) and the LDD-TP–R for the two-domain case. The consistency of the solver is theoretically shown.

2.1 | Coupling the full two-phase flow model with the Richards equation: The TP–R model

Let a Lipschitz domain $\Omega \subset \mathbb{R}^d$, $d \in \{2, 3\}$, be decomposed into two non-overlapping Lipschitz subdomains $\Omega_1, \Omega_2 \subset \mathbb{R}^d$ such that $\Omega = \Omega_1 \cup \Gamma \cup \Omega_2$, with $\Gamma := \left(\overline{\Omega_1} \cap \overline{\Omega_2}\right) \setminus \partial\Omega$ being the interface.

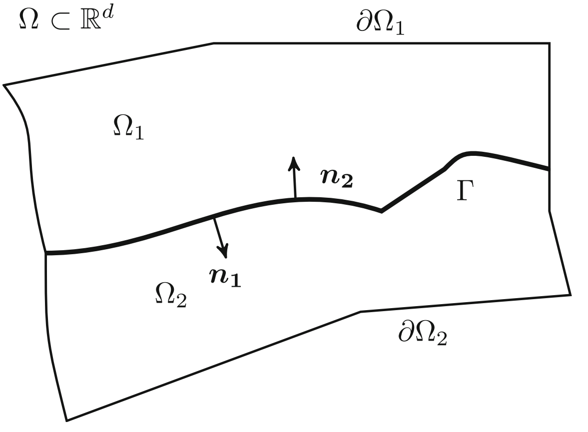

FIGURE 1 Illustration of a layered soil domain $\Omega = \Omega_1 \cup \Omega_2 \cup \Gamma \subset \mathbb{R}^d$ with fixed interface Γ. For the upper domain Ω_1 we use the Richards equation whereas the full two-phase model applies in Ω_2. The normals $\mathbf{n}_{1,2}$ point out of the respective domains

The latter is assumed to be a $(d-1)$-dimensional Lipschitz manifold. By $\mathbf{n_1}, \mathbf{n_2}$ we denote the outer normals on the intersection of Γ and the boundaries of Ω_1, Ω_2. We refer to Figure 1 for a sketch of the described situation. The entire domain Ω is filled by a porous medium which is assumed to be isotropic on each subdomain. We consider the dynamics of two immiscible, incompressible and viscous fluids, denoted as a wetting one (w) and a nonwetting one (nw). Considering a hybrid ansatz we suppose the full two-phase model to be valid in domain Ω_2, compare [26, 27], whereas we assume that on Ω_1 the simplified Richards model, compare [28, 29], is justified. A typical situation in which this occurs is the flow of water and air through a porous medium that is so permeable that the air phase can be considered to be "infinitely" mobile, resulting in a constant air pressure field equal to the atmospheric pressure. In view of the model hierarchy discussed for example, in [30], the Richards model can be also viewed as the limit of a two-phase flow regime if the ratio of the nonwetting and the wetting viscosity tends to zero (and hence the mobility to infinity). With this interpretation, other situations than water and air are conceivable for a hybrid model ansatz.

Precisely, we consider the following coupling of the Richards equation with the two-phase flow model in pressure–pressure formulation.

Problem 1 (TP–R problem) For $l \in \{1,2\}$, let $\Omega_{l,T} := \Omega_l \times (0,T)$ and $\Gamma_T := \Gamma \times (0,T)$. The coupled two-phase– Richards (TP–R) problem consists of finding phase pressures $p_{w,1}, p_{w,2}$ and $p_{nw,2}$ solving

$$\Phi_1 \partial_t S_1 \left(p_a, p_{w,1}\right) - \nabla \cdot \left(\frac{k_{\mathrm{i},1}}{\mu_w} k_{w,1}\left(S_1\right) \nabla \left(p_{w,1} + z_w\right)\right) = f_{w,1} \tag{1}$$

in $\Omega_{1,T}$ together with

$$\Phi_2 \partial_t S_2 \left(p_{nw,2}, p_{w,2}\right) - \nabla \cdot \left(\frac{k_{\mathrm{i},2}}{\mu_w} k_{w,2}\left(S_2\right) \nabla \left(p_{w,2} + z_w\right)\right) = f_{w,2}, \tag{2}$$

$$-\Phi_2 \partial_t S_2 \left(p_{nw,2}, p_{w,2}\right) - \nabla \cdot \left(\frac{k_{\mathrm{i},2}}{\mu_{nw}} k_{nw,2}\left(1 - S_2\right) \nabla \left(p_{nw,2} + z_{nw}\right)\right) = f_{nw,2} \tag{3}$$

in $\Omega_{2,T}$. Equations (1)–(3) are coupled via

$$
\begin{aligned}
p_{w,1} &= p_{w,2}, & \boldsymbol{F_{w,1}} \cdot \boldsymbol{n_1} &= \boldsymbol{F_{w,2}} \cdot \boldsymbol{n_1}, \\
p_{nw,2} &= p_a, & \boldsymbol{F_{nw,2}} \cdot \boldsymbol{n_2} &= \boldsymbol{F_{nw,1}} \cdot \boldsymbol{n_2}
\end{aligned} \tag{4}
$$

on Γ_T. The problem is closed by suitable initial as well as boundary conditions.

We proceed to explain the notation used in Problem 1 including the specification of the fluxes in (4). For subdomain index $l \in \{1, 2\}$, our primary unknowns are the wetting pressure $p_{w,l}$ and the nonwetting pressure $p_{nw,l}$ on $\Omega_{l,T}$, respectively. The given constant atmospheric pressure is denoted by p_a and on $\Omega_{1,T}$, we have $p_{nw,1} = p_a$, by assumption. The functions $S_l = S_l\left(p_{nw,l}, p_{w,l}\right) \in [0, 1]$ denote the wetting saturations and are assumed to be functions of the phase pressures via the capillary pressure saturation relationships $p_{c,l}(S_l) = p_{nw,l} - p_{w,l}$, see for example, [26], that is, it is assumed that the functions $p_{c,l}$ are invertible, compare Assumption 1. Since we model two-phase flow, we use the assumption that on all subdomains Ω_l only the two phases are present, that is, the nonwetting saturations S_l^{nw} can be expressed by the relations $S_l^{nw} = 1 - S_l$. This is already built into the equation (3).

The porosities $\Phi_l \in (0, 1)$ on each subdomain Ω_l are assumed to be constant and furthermore, we denote by $\rho_\alpha > 0$ the density and by $\mu_\alpha > 0$ the viscosity of phase $\alpha \in \{w, nw\}$. For simplicity, we assume that the intrinsic permeabilities $\boldsymbol{K_l}$ are isotropic on every subdomain, that is, $\boldsymbol{K_l} = k_{\mathrm{i},l}\boldsymbol{E_d}$. Finally, for $\alpha \in \{w, nw\}$, $k_{\alpha,l}$ denotes the given relative permeability, $f_{\alpha,l}$ a source term and $z_\alpha = \rho_\alpha g x_d$ is the gravitational force term (g being the gravitational acceleration).

The fluxes in (4) determine the mass flow coupling between the domains. For $(\alpha, l) \in \{(w, 1), (w, 2), (nw, 2)\}$ they are given by

$$
\boldsymbol{F}_{\alpha,\mathbf{l}} = -\frac{k_{\mathrm{i},l}}{\mu_\alpha} k_{\alpha,l}(S_l)\, \nabla \left(p_{\alpha,l} + z_\alpha\right). \tag{5}
$$

It remains to determine the flux $\boldsymbol{F_{nw,1}}$. When coupling the Richards model with the two-phase flow equations, it is not clear which conditions should be imposed in (4), because the nonwetting phase is considered to be present, yet remains unmodelled. Since on Ω_1 the nonwetting pressure is assumed to be constant, $p_{nw,l} = p_a$, the part of the nonwetting Neumann flux containing the gradient of the pressure (in a two-phase flow model) would have to vanish. However, this is not the case for the gravitational part. Thus, there are two possible ways to account for the gravitational force of the nonwetting phase on Ω_1 at the interface. In view of the fact that the Richards model is the mathematical limit of the two-phase model, compare [30], one choice is

$$
\boldsymbol{F_{nw,1}} = \frac{k_{\mathrm{i},1}}{\mu_{nw}} k_{nw,1}\left(1 - S_1\left(p_a, p_{w,1}\right)\right) \nabla z_{nw}. \tag{6}
$$

On the other hand, one could ignore the effect entirely, that is,

$$
\boldsymbol{F_{nw,1}} = \mathbf{0}. \tag{7}
$$

The two coupling relations (6) and (7) are suggested in an adhoc manner. A rigorous derivation of coupling conditions via e.g. homogenization techniques is out of the scope of the present paper. However, we point out that the formulation of the LDD scheme and its proof of convergence work for both cases.

Remark 1 (Extended coupling conditions) The coupling conditions in Problem 1 are the generic domain decomposition coupling conditions providing equivalence of the substructured problem to a monodomain formulation. While natural in this sense, they exhibit certain limitations from a modeling perspective. Indeed, since we prescribe the continuity of the phase pressures, the capillary pressures are continuous as well.

However, in general, capillary trapping phenomena can occur for heterogeneous soils, where a phase might not enter into another soil layer due to a pressure barrier. This translates to a pressure jump over the interface. Nonmatching capillary pressure curves that in addition are extended to multivalued functions for vanishing (wetting or nonwetting) saturations, need to be considered in this case, compare [31]. This approach reflects pressure discontinuities over the interface by imposing the continuity of the capillary pressures together with the continuity of the wetting pressure in a generalized, multivalued sense. However, the analytical treatment (proof of existence of solutions) of this generalized formulation consists in approximating nonmatching capillary pressure curves by a family of matching curves with continuous phase pressures.

From the numerical point of view it is therefore important to investigate the applicability of the LDD solver to the case of continuous pressures not only as a first step, but notably so as an approximation of the more realistic discontinuous case. We refer to [17] for a recent contribution in this direction.

2.2 | Function spaces

Before we give the weak formulation for Problem 1 we introduce some notions for function spaces on Lipschitz domains and their boundaries, the latter being essential for the analysis of the transmission conditions in the domain decomposition method. In this section, $\Omega \subset \mathbb{R}^d$ denotes a generic Lipschitz domain. In particular, all notations apply to all domains Ω, Ω_l, $l = 1, 2$ introduced in the previous sections. Spaces on Ω. $C_0^\infty(\Omega)$ denotes the space of smooth functions with compact support in Ω. $L^2(\Omega)$ is the space of square-integrable functions equipped with the scalar product $\langle \cdot, \cdot \rangle$. For $s \in \mathbb{R}$, the space $H^s\left(\mathbb{R}^d\right)$ denotes the standard Sobolev-Slobodeckij space with norm $\|u\|_{H^s(\Omega)}$. We will need $H_0^1(\Omega) = \overline{C_0^\infty(\Omega)}^{H^1}$, and for vector-valued functions $v : \Omega \to \mathbb{R}^d$, the space

$$H(\mathrm{div}, \Omega) := \left\{ v \in \left[L^2(\Omega)\right]^d \,\middle|\, \mathrm{div} v \in L^2(\Omega) \right\},$$

together with the norm $\|v\|^2_{H(\mathrm{div},\Omega)} := \|v\|^2_{L^2} + \|\mathrm{div} v\|^2_{L^2}$, $\mathrm{div} v$ being understood via the integration by parts formula.

SPACES On $\Gamma \subset \partial\Omega$. The spaces $H^s(\Gamma)$ for $|s| \leq 1$ are defined by understanding that functions on $\partial\Omega$ in local coordinates belong to $H^s\left(\mathbb{R}^{d-1}\right)$. When the Lipschitz surface $\partial\Omega$ is divided into two surfaces Γ_1 and Γ_2, $\partial\Omega = \Gamma_1 \cup \partial\Gamma_j \cup \Gamma_2$, with their common boundaries $\partial\Gamma_j$ of dimension $d-2$ in turn being Lipschitz, the spaces $H^s\left(\Gamma_j\right)$ for $|s| \leq 1$ can be introduced in the same way.

For a function $u \in H^{1/2}\left(\Gamma_j\right)$ the extension $\tilde{\cdot}$ by zero on $\partial\Omega \backslash \Gamma_j$ does not imply $u \in H^{1/2}(\partial\Omega)$, see [6, Theorem 3.4.4] and the discussion thereafter. In order to define Neumann traces in a generalized sense via the Green formula on parts of the boundary, we need to define the subspace of those functions in $H^{1/2}(\Gamma)$ for which the extension by zero belongs to $H^{1/2}(\partial\Omega)$, that is

$$H_{00}^{1/2}(\Gamma) := \left\{ u \in H^{1/2}(\Gamma) \,|\, \widetilde{u} \in H^{1/2}(\partial\Omega) \right\}, \qquad \|u\|_{H_{00}^{1/2}(\Gamma)} := \|\widetilde{u}\|_{H^{1/2}(\partial\Omega)}.$$

With the scalar product inherited from $H^{1/2}(\partial\Omega)$ the space $H_{00}^{1/2}(\Gamma)$ becomes a Hilbert space.

With these definitions, the trace operator $\gamma_\Gamma : H^1(\Omega) \to H^{1/2}(\Gamma)$ can be defined as extension of the restriction on smooth functions, acting as a bounded, surjective linear operator on these spaces with bounded right inverse $\mathcal{R}_\Gamma : H^{1/2}(\Gamma) \to H^1(\Omega)$, compare [32, Theorem A.2.3 and p. 132 ff], [6, Theorem 9.2.1, p. 118] or [33, 34]. To ease the notation, we will denote the trace by $u|_\Gamma$ instead of $\gamma_\Gamma u$. Moreover, there is a unique linear continuous operator $\gamma^{\boldsymbol{n}}_{\partial\Omega} : H(\mathrm{div}, \Omega) \to H^{-1/2}(\Gamma)$ such that $\gamma^{\boldsymbol{n}} u = (u \cdot \boldsymbol{n})|_\Gamma$ for $u \in H(\mathrm{div}, \Omega) \cap [C(\overline{\Omega})]^d$. It is in this generalized sense that we will understand Neumann fluxes.

DUAL SPACES. Denoting the dual spaces $\mathcal{L}(H^s, \mathbb{R})$ equipped with the standard norm by $H^{s\prime}$, functionals $F \in H^{s\prime}$ can be identified via the Riesz representation theorem as an element of $v_F \in H^s$ itself, that is, $F(u) = \langle v_F, u\rangle_{H^s}$ for $u \in H^s$ and $\langle \cdot, \cdot \rangle_{H^s}$ denoting the scalar product. However, extending the form $(u, v)_{\mathbb{R}^d} := \langle u, v\rangle_{H^0(\mathbb{R}^d)}$ to $H^{-s}\left(\mathbb{R}^n\right) \times H^s\left(\mathbb{R}^d\right)$ renders the spaces $H^{-s}\left(\mathbb{R}^d\right)$ and $H^s\left(\mathbb{R}^d\right)$ mutually dual, providing an alternative representation of functionals on H^s, compare [6, p. 9 ff]. A similar duality holds for H^s-spaces on Ω and $\Gamma \subset \partial\Omega$, see [6, Theorem 5.1.12, p. 61]. For the case $s = \frac{1}{2}$ which we need here, we have $H^{1/2}_{00}(\Gamma)' = H^{-1/2}(\Gamma)$ for $\Gamma \subset \partial\Omega$. We will use the symbol $\langle \cdot, \cdot \rangle_\Gamma$ for the evaluation $F(\varphi)$ of a functional $F \in H^{-1/2}(\Gamma)$ with a function $\varphi \in H^{1/2}_{00}(\Gamma)$ also referred to as dual pairing.

Remark 2 Note that the considerations on duality from above show that each functional u in $H^{1/2}_{00}(\Gamma)'$ has two representations. Namely, there is a function $\hat{u} \in H^{-1/2}(\Gamma)$ and another function $\bar{u} \in H^{1/2}_{00}(\Gamma)$ such that

$$\langle u, \varphi\rangle_\Gamma = \langle \hat{u}, \varphi\rangle_{H^0(\Gamma)} \text{ and } \langle u, \varphi\rangle_\Gamma = \langle \bar{u}, \varphi\rangle_{H^{1/2}_{00}(\Gamma)}. \tag{8}$$

hold. The choice of representation will be important in the formulation of the domain decomposition scheme below.

2.3 | The LDD-TP–R solver for the TP–R problem

In this section we introduce a time-discrete weak formulation of Problem 1 and formulate an LDD solver for this setting. Based on Section 2.2 we define spaces associated to the subdomain partition. For $l \in \{1, 2\}$, we define

$$\mathcal{V}_l := \left\{u \in H^1\left(\Omega_l\right) \mid u|_{\partial\Omega_l \cap \partial\Omega} \equiv 0\right\} \text{ and } \mathcal{V} := \left\{(u_1,\ u_2) \in \mathcal{V}_1 \times \mathcal{V}_2 \mid u_1|_\Gamma \equiv u_2|_\Gamma\right\},$$

where the norms in the spaces $\mathcal{V}_l$ are the standard $H^1\left(\Omega_l\right)$-norms, and on $\mathcal{V}$ the norm $\|\cdot\|^2_{\mathcal{V}} = \sum_{l=1,2} \|\cdot\|^2_{\mathcal{V}_l}$ is used. $\mathcal{V}_{l'}$ denotes again the dual space of $\mathcal{V}_l$ and is equipped with the usual norm for functionals $\|F\|_{\mathcal{V}_{l'}} = \sup_{\varphi_l \in \mathcal{V}_l} \frac{\|F\varphi_l\|_{\mathcal{V}_l}}{\|\varphi_l\|_{\mathcal{V}_l}}$.

Remark 3 Henceforth, we assume that the atmospheric pressure p_a vanishes. This can be done without loss of generality: let $\widetilde{p}$ be a physical pressure and $\widetilde{p}_a$ the atmospheric pressure. By introducing $p := \widetilde{p} - \widetilde{p}_a$, the desired normalization $p_a = 0$ is achieved and (1), (2), (3) stay the same, since $Dp = D\widetilde{p}$ for all derivatives and $p_c^{-1}\left(\widetilde{p}_{nw} - \widetilde{p}_w\right) = S = p_c^{-1}\left(\widetilde{p}_{nw} - \widetilde{p}_a - \left(\widetilde{p}_w - \widetilde{p}_a\right)\right) = p_c^{-1}\left(p_{nw} - p_w\right)$.

As a consequence the nonwetting pressure unknown in the two-phase model domain Ω_2 at a discrete time step will be in $H^1_0\left(\Omega_2\right)$ and not in the space $\mathcal{V}_2$.

As the first step toward the LDD solver, we formulate a time discrete version of Problem 1. For $N \in \mathbb{N}$, the introduction of the time step size $\tau := \frac{T}{N}$ partitions the interval $[0, T]$ into the $N + 1$ time steps $t^n := n \cdot \tau, n = 0, \ldots, N$.

The functions $p^n_{w,1} : \Omega_1 \to \mathbb{R}$ and $p^n_{w,2},\ p^n_{nw,2} : \Omega_2 \to \mathbb{R}$ denote the unknown time-discrete pressures at time step t^n. In addition, we set $S^n_l = S_l\left(p^n_{nw,l}, p^n_{w,l}\right)$(anticipating $p^n_{nw,1} = p_a = 0$) and abbreviate

$$k^n_{w,l} := \frac{k_{i,l}}{\mu_w} k_{w,l}\left(S^n_l\right), \quad k^n_{nw,l} := \frac{k_{i,l}}{\mu_{nw}} k_{nw,l}\left(1 - S^n_l\right). \tag{9}$$

Consequently the fluxes at t^n write as

$$\mathbf{F}^{\boldsymbol{n}}_{\boldsymbol{w,l}} := -k^n_{w,l}\nabla\left(p^n_{w,l} + z_w\right), l \in \{1,2\} \text{ and } \mathbf{F}^{\boldsymbol{n}}_{\boldsymbol{nw,2}} := -k^n_{nw,2}\nabla\left(p^n_{nw,2} + z_{nw}\right).$$

Depending on the choices in (6) and (7) the time-discrete flux $\mathbf{F}^{\boldsymbol{n}}_{\boldsymbol{nw,1}}$ is defined in the same way.

With a backward Euler discretization in time, the time-discrete coupled TP–R problem in weak form then reads as follows.

Problem 2 (Time-discrete TP–R problem) For some $n \in \mathbb{N}$, let $\left(p^{n-1}_{w,1}, p^{n-1}_{w,2}\right) \in \mathcal{V}$ and $p^{n-1}_{nw,2} \in H^1_0(\Omega_2)$. Then, the time-discrete TP–R problem consists of finding $\left(\left(p^n_{w,1}, p^n_{w,2}\right), p^n_{nw,2}\right) \in \mathcal{V} \times H^1_0(\Omega_2)$, such that $\mathbf{F}^{\boldsymbol{n}}_{\boldsymbol{\alpha,l}} \cdot \boldsymbol{n_l} \in H^{1/2}_{00}(\Gamma)'$ holds for $l = 1,2$, $\alpha \in \{n, nw\}$ and such that the equations

$$\left\langle \Phi_1 S^n_1 - \Phi_1 S^{n-1}_1, \varphi_{w,1}\right\rangle - \tau\left\langle \boldsymbol{F}^{\boldsymbol{n}}_{\boldsymbol{w,1}}, \nabla\varphi_{w,1}\right\rangle + \tau\left\langle \boldsymbol{F}^{\boldsymbol{n}}_{\boldsymbol{w,2}} \cdot \boldsymbol{n_1}, \varphi_{w,1}\right\rangle_\Gamma = \tau\left\langle f^n_{w,1}, \varphi_{w,1}\right\rangle, \tag{10}$$

$$\left\langle \Phi_2 S^n_2 - \Phi_2 S^{n-1}_2, \varphi_{w,2}\right\rangle - \tau\left\langle \boldsymbol{F}^{\boldsymbol{n}}_{\boldsymbol{w,2}}, \nabla\varphi_{w,2}\right\rangle + \tau\left\langle \boldsymbol{F}^{\boldsymbol{n}}_{\boldsymbol{w,1}} \cdot \boldsymbol{n_2}, \varphi_{w,2}\right\rangle_\Gamma = \tau\left\langle f^n_{w,2}, \varphi_{w,2}\right\rangle, \tag{11}$$

$$-\left\langle \Phi_2 S^n_2 - \Phi_2 S^{n-1}_2, \varphi_{nw,2}\right\rangle - \tau\left\langle \boldsymbol{F}^{\boldsymbol{n}}_{\boldsymbol{nw,2}}, \nabla\varphi_{nw,2}\right\rangle + \tau\left\langle \boldsymbol{F}^{\boldsymbol{n}}_{\boldsymbol{nw,1}} \cdot \boldsymbol{n_2}, \varphi_{nw,2}\right\rangle_\Gamma = \tau\left\langle f^n_{nw,2}, \varphi_{nw,2}\right\rangle \tag{12}$$

are satisfied for all $\left(\varphi_{w,1}, \varphi_{w,2}\right) \in \mathcal{V}_1 \times \mathcal{V}_2$ and $\varphi_{nw,2} \in \mathcal{V}_2$.

Remark 4 (i) In what follows, we will assume, that there is a unique solution $\left(\left(p^n_{w,1}, p^n_{w,2}\right), p^n_{nw,2}\right) \in \mathcal{V} \times H^1_0(\Omega_2)$ for the nonlinear time-discrete Problem 2. We are not aware of any results concerning its well-posedness but we expect that an analytic fixed point iteration combining existence results from linear elliptic theory and Schauder's or Banach's fixed point theorem can be applied.
ii) Note that traces of functions are implicitly taken in (10)–(12). They are needed for the dual pairings of functionals on Γ or likewise the scalar product of spaces on Γ, that is, $\langle u, \varphi\rangle_\Gamma = \langle u\,|_\Gamma, \varphi|_\Gamma\rangle_\Gamma$ if $u, \varphi \in \mathcal{V}_l$.

For each solution $\left(\left(p^n_{w,1}, p^n_{w,2}\right), p^n_{nw,2}\right)$ of Problem 2 the coupling conditions (4) are implicitly fulfilled in a weaker form at each time step t_n. Namely, we have $p^n_{w,1}\Big|_\Gamma = p^n_{w,2}\Big|_\Gamma$ and $p^n_{nw,2}\Big|_\Gamma = 0$ in the sense of traces by the definition of the spaces $\mathcal{V}$, and $H^1_0(\Omega_2)$. The continuity of the fluxes, $\mathbf{F}^{\boldsymbol{l}}_{\boldsymbol{\alpha,l}} \cdot \boldsymbol{n_l} = \boldsymbol{F}^{\boldsymbol{n}}_{\boldsymbol{\alpha,3-l}} \cdot \boldsymbol{n_l}$, $\alpha \in \{w, nw\}$, is given as equality of functionals in $H^{1/2}_{00}(\Gamma)'$. This is true regardless of the different choices for $\boldsymbol{F}^{\boldsymbol{n}}_{\boldsymbol{nw,1}}$.

Next, we define the iterative domain decomposition ansatz with iteration number $i \in \mathbb{N}_0$ based on the time-discrete TP–R problem in weak formulation. Extending the notation once more, the functions $p^{n,i}_{w,1} : \Omega_1 \to \mathbb{R}$ and $p^{n,i}_{w,2}, p^{n,i}_{nw,2} : \Omega_2 \to \mathbb{R}$ denote the unknown ith pressure iterate during the solving for pressures of time step t^n. We set again $S^{n,i}_l = S_l\left(p^{n,i}_{nw,l}, p^{n,i}_{w,l}\right)$ using $p^{n,i}_{nw,1} = p_a = 0$. With the notations

$$k^{n,i}_{w,l} := \frac{k_{\mathrm{i},l}}{\mu_w} k_{w,l}\left(S^{n,i}_l\right), \qquad k^{n,i}_{nw,l} := \frac{k_{\mathrm{i},l}}{\mu_{nw}} k_{nw,l}\left(1 - S^{n,i}_l\right), \tag{13}$$

the flux iterates at t^n are given by

$$\mathbf{F}^{\boldsymbol{n,i}}_{\boldsymbol{w,l}} := -k^{n,i-1}_{w,l}\nabla\left(p^{n,i}_{w,l} + z_w\right), \; l \in \{1,2\} \quad \text{and} \quad \boldsymbol{F}^{\boldsymbol{n,i}}_{\boldsymbol{nw,2}} := -k^{n,i-1}_{nw,2}\nabla\left(p^{n,i}_{nw,2} + z_{nw}\right).$$

The flux iterate $\boldsymbol{F}^{\boldsymbol{n,i}}_{\boldsymbol{nw,1}}$ is defined case by case in the same way.

LDD schemes are designed to address simultaneously the two main challenges of Problem 2. Firstly, each equation in Problem 2 is doubly nonlinear, nonlinearities being present in the discretized time derivative, as well as in the fluxes. Secondly, the system of equations (10) to (12) is nonlinearly coupled and the coupling conditions contain nonlinearities themselves. The LDD method tackles both of these problems by linearizing and decoupling the equations in one single fixed point iteration.

We assume that $\left(\left(p_{w,1}^{n-1}, p_{w,2}^{n-1}\right), p_{nw,2}^{n-1}\right) \in \mathcal{V} \times H_0^1(\Omega_2)$ is given and set as initial iterates in the nth time step

$$p_{w,l}^{n,0} := p_{w,l}^{n-1} \quad \text{on} \quad \Omega_l, \quad l = 1, 2, \quad \text{and} \quad p_{nw,2}^{n,0} := p_{nw,2}^{n-1}, \quad \text{on} \quad \Omega_2, \tag{14}$$

Let the numbers $\lambda_\alpha \in (0, \infty)$, $\alpha \in \{n, nw\}$ be given. They are introduced to control the ratio between Dirichlet and flux-type transmission conditions. Following Lions, [3, 35], we introduce the Robin-type interface terms

$$g_{\alpha,l}^0 := \mathbf{F}_{\alpha,l}^{n-1} \cdot \boldsymbol{n}_l - \lambda_\alpha p_{\alpha,l}^{n-1}\Big|_\Gamma \tag{15}$$

as functionals in $H_{00}^{1/2}(\Gamma)'$ for both phases and both subdomains. Since on Ω_1 the nonwetting pressure is constant, $p_{nw,1} = p_a = 0$, we define either

$$g_{nw,1}^0 := \boldsymbol{F}_{nw,1}^{n-1} \cdot \boldsymbol{n}_1 = k_{nw,1}^{n-1} \nabla z_{nw} \cdot \boldsymbol{n}_1 \tag{16}$$

if gravity effects are included, corresponding to the right hand side of (6), or

$$g_{nw,1}^0 := \boldsymbol{F}_{nw,1}^{n-1} \cdot \boldsymbol{n}_1 = 0 \tag{17}$$

instead, in case gravity effects are excluded, as is expressed through the right hand side of (7).

Note 1 (Pressure functionals) For $p \in \mathcal{V}_l$, we define the pressure functionals $\langle p, \cdot \rangle_\Gamma \in H_{00}^{1/2}(\Gamma)'$ on the interface such as the ones appearing in (15) according to

$$\langle p, \cdot \rangle_\Gamma := \langle p, \cdot \rangle_{1/2}. \tag{18}$$

In this way, the pressure traces $p|_\Gamma$ are representing the functionals $\langle p, \cdot \rangle_\Gamma \in H_{00}^{1/2}(\Gamma)'$ w.r.t the $H_{00}^{1/2}(\Gamma)$-scalar product, that is, $p|_\Gamma = \overline{p}$, compare Remark 2. This will be important in the proof of Theorem 1.

Now, the LDD -TPR scheme approximates the solution to the time-discrete Problem 2 at time t_n by solving subsequently the following problem (LDD-TPR solver), together with the initial iterates given in (14) and (15).

Problem 3 (LDD-TP–R solver) *Let* $L_{w,2}, L_{nw,2}, L_{w,1} > 0$ and some previously known iterates $p_{\alpha,l}^{n,i-1} \in \mathcal{V}_l$, $g_{\alpha,l}^{i-1} \in H_{00}^{1/2}(\Gamma)'$ be given for $i \in \mathbb{N}, n \geq 1$.
Find $\left(p_{w,1}^{n,i}, p_{w,2}^{n,i}, p_{nw,2}^{n,i}\right) \in \mathcal{V}_1 \times \mathcal{V}_2 \times \mathcal{V}_2$, such that

$$L_{w,l} \left\langle p_{w,l}^{n,i}, \varphi_{w,l} \right\rangle - \tau \left\langle \boldsymbol{F}_{w,l}^{n,i}, \nabla \varphi_{w,l} \right\rangle + \tau \left\langle \lambda_w p_{w,l}^{n,i} + g_{w,l}^i, \varphi_{w,l} \right\rangle_\Gamma$$

$$= L_{w,l} \left\langle p_{w,l}^{n,i-1}, \varphi_{w,l} \right\rangle - \left\langle \Phi_l S_l^{n,i-1} - \Phi_l S_l^{n-1}, \varphi_{w,l} \right\rangle + \tau \left\langle f_{w,l}^n, \varphi_{w,l} \right\rangle \tag{19}$$

is fulfilled for $l \in \{1, 2\}$ with

$$\left\langle g_{w,l}^i, \varphi_{w,l} \right\rangle_\Gamma := \left\langle -2\lambda_w p_{w,3-l}^{n,i-1} - g_{w,3-l}^{i-1}, \varphi_{w,l} \right\rangle_\Gamma, \tag{20}$$

as well as

$$L_{nw,2}\left\langle p^{n,i}_{nw,2},\varphi_{nw,2}\right\rangle-\tau\left\langle \boldsymbol{F}^{n,i}_{nw,2},\nabla\varphi_{nw,2}\right\rangle+\tau\left\langle \lambda_{nw}p^{n,i}_{nw,2}+g^{i}_{nw,2},\varphi_{nw,2}\right\rangle_{\Gamma}$$

$$=L_{nw,2}\left\langle p^{n,i-1}_{nw,2},\varphi_{nw,2}\right\rangle+\left\langle \Phi_2S^{n,i-1}_{2}-\Phi_2S^{n-1}_{2},\varphi_{nw,2}\right\rangle+\tau\left\langle f^{n}_{nw,2},\varphi_{nw,2}\right\rangle \tag{21}$$

with

$$\left\langle g^{i}_{nw,1},\varphi_{nw,2}\right\rangle_{\Gamma}:=\left\langle -2\lambda_{nw}p^{n,i-1}_{nw,2}-g^{i-1}_{nw,2},\varphi_{nw,2}\right\rangle_{\Gamma}, \tag{22}$$

$$\left\langle g^{i}_{nw,2},\varphi_{nw,2}\right\rangle_{\Gamma}:=\left\langle -g^{i-1}_{nw,1},\varphi_{nw,2}\right\rangle_{\Gamma}, \tag{23}$$

for all $\varphi_{w,1}\in\mathcal{V}_1$, $\varphi_{w,2}\in\mathcal{V}_2$ and $\varphi_{nw,2}\in\mathcal{V}_2$.

Notice that in a two-domain situation the index of the adjacent domain can be denoted by $3-l$, for any given $l\in\{1,2\}$, since $3-l=2$ for $l=1$ and $3-l=1$ for $l=2$. This type of notation has been used in Problem 3 and will be used henceforth.

Remark 5 It may look peculiar to introduce an update for the term $g^{i}_{nw,1}$ in (22) and (23) as we do not have any equation for the nonwetting phase on Ω_1. However, it is precisely this way of updating the $g^{i}_{\alpha,l}$ terms, that liberates the nonwetting pressure iterates $p^{n,i}_{nw,2}$ of the requirement to being elements of $H^1_0(\Omega_2)$, that is, to fulfill continuity to the atmospheric pressure *in each iteration*. Instead, it allows to merely require that $p^{n,i}_{nw,2}$ is an element of $\mathcal{V}_2$. This is less restrictive. In the present formulation, the LDD solver enforces $p^{n,i}_{nw,2}\big|_{\Gamma}\to 0$ in the limit $i\to\infty$ all by itself. Moreover, it enables us to formulate a scheme that treats both model assumptions (6) and (7) in a unified manner.

The assertions of Remark 5 will be verified once Problem 2 is reformulated such that the reformulation can be recognized as the formal limit system of the solver and the convergence of the LDD-TP–R solver to this reformulation is proven. The reformulation of Problem 2 is given in the next section.

2.4 | Consistency of the LDD-TP–R solver with the time-discrete TP–R Problem 2

Recall that for a solution $\left(\left(p^{n}_{w,1},p^{n}_{w,2}\right),p^{n}_{nw,2}\right)\in\mathcal{V}\times H^1_0(\Omega_2)$ of Problem 2 the nonwetting Neumann flux $\boldsymbol{F}^{n}_{nw,1}\cdot\boldsymbol{n}_1$ is defined by the right hand side of either (6) or (7), compare also (17) and (16). Thus, the functionals

$$g_{w,l}:=-\lambda_w p^{n}_{w,l}\big|_{\Gamma}+\boldsymbol{F}^{n}_{w,l}\cdot\boldsymbol{n}_l \quad (l=1,2), \tag{24}$$

$$g_{nw,1}:=-\lambda_{nw}\underbrace{p^{n}_{nw,1}\big|_{\Gamma}}_{=p_a=0}+\boldsymbol{F}^{n}_{nw,1}\cdot\boldsymbol{n}_1 \quad\text{and}\quad g_{nw,2}:=-\lambda_{nw}\underbrace{p^{n}_{nw,2}\big|_{\Gamma}}_{=0}+\boldsymbol{F}^{n}_{nw,2}\cdot\boldsymbol{n}_2, \tag{25}$$

in $H^{1/2}_{00}(\Gamma)'$ fulfill the relations

$$g_{w,l}=-2\lambda_w p^{n}_{w,3-l}\big|_{\Gamma}+\lambda_w p^{n}_{w,3-l}\Big|_{\Gamma}-\boldsymbol{F}^{n}_{w,3-l}\cdot\boldsymbol{n}_{3-l}=-2\lambda_w p^{n}_{w,3-l}\Big|_{\Gamma}-g_{w,3-l}\quad (l=1,2),$$

$$g_{nw,1}=-2\lambda_{nw}p^{n}_{nw,2}\big|_{\Gamma}-g_{nw,2}\quad\text{and}\quad g_{nw,2}=-g_{nw,1}.$$

Note that $p^n_{w,1}\Big|_\Gamma = p^n_{w,2}\Big|_\Gamma$, $p^n_{nw,2}\Big|_\Gamma = 0$ and $\boldsymbol{F_{\alpha,1}} \cdot \boldsymbol{n_1} = -\boldsymbol{F_{\alpha,2}} \cdot \boldsymbol{n_2}$ for $\alpha \in \{w, nw\}$. Problem 2 can therefore be written as

$$\left\langle \Phi_l S^n_l - \Phi_l S^{n-1}_l, \varphi_{w,l} \right\rangle - \tau \left\langle \mathbf{F}^{\boldsymbol{n}}_{\boldsymbol{w,l}}, \nabla\varphi_{w,l} \right\rangle + \tau \left\langle \lambda_w p^n_{w,l} + g_{w,l}, \varphi_{w,l} \right\rangle_\Gamma = \tau \left\langle f^n_{w,l}, \varphi_{w,l} \right\rangle \tag{19$'$}$$

with

$$\langle g_{w,l}, \varphi_{w,l} \rangle_\Gamma = \left\langle -2\lambda_w p^n_{w,3-l} - g_{w,3-l}, \varphi_{w,l} \right\rangle_\Gamma, \tag{20$'$}$$

for $l \in \{1,2\}$ as well as

$$-\left\langle \Phi_2 S^n_2 - \Phi_2 S^{n-1}_2, \varphi_{nw,2} \right\rangle - \tau \left\langle \boldsymbol{F}^{\boldsymbol{n}}_{\boldsymbol{nw,2}}, \nabla\varphi_{nw,2} \right\rangle + \tau \left\langle \lambda_{nw} p^n_{nw,2} + g_{nw,2}, \varphi_{nw,2} \right\rangle_\Gamma = \tau \left\langle f^n_{nw,2}, \varphi_{nw,2} \right\rangle \tag{21$'$}$$

together with

$$\langle g_{nw,1}, \varphi_{nw,2} \rangle_\Gamma = \left\langle -2\lambda_{nw} p^n_{nw,2} - g_{nw,2}, \varphi_{nw,2} \right\rangle_\Gamma, \tag{22$'$}$$

$$\langle g_{nw,2}, \varphi_{nw,2} \rangle_\Gamma = \langle -g_{nw,1}, \varphi_{nw,2} \rangle_\Gamma. \tag{23$'$}$$

We know $p^n_{nw,2}\Big|_\Gamma = 0$ since $p^n_{nw,2} \in H^1_0(\Omega_2)$ and thus the pressure functionals in (21′)–(22′) actually disappear. They are written out here to emphasize the structure.

Conversely, any tuple of functions $\left(p^n_{w,1}, p^n_{w,2}, p^n_{nw,2}\right) \in \mathcal{V}_1 \times \mathcal{V}_2 \times \mathcal{V}_2$ fulfilling (19′) – (23′) together with

$$g_{nw,1} = \boldsymbol{F}^{\boldsymbol{n}}_{\boldsymbol{nw,1}} \cdot \boldsymbol{n_1}, \tag{26}$$

where $\boldsymbol{F}^{\boldsymbol{n}}_{\boldsymbol{nw,1}} \cdot \boldsymbol{n_1}$ is defined by the right hand side of either (6) or (7), is a solution of Problem 2.

The argument supporting this claim for the wetting phase has been given in the proof of [1, Lemma 2] or [36, Lemma 2.3.12] and it carries over to the situation here.

Regarding the nonwetting phase on Ω_2, notice that $p^n_{nw,2}\Big|_\Gamma = 0$ is contained in (23) and (22) as $\left\langle p^n_{nw,2}, \varphi_{nw,2} \right\rangle_\Gamma = 0$ follows for all $\varphi_{nw,2} \in \mathcal{V}_2$ by plugging (23′) into (22′). By our definition of the pressure functionals, compare Note 1, as well as by virtue of the surjectivity of the trace operator, this means $\left\langle p^n_{nw,2}\Big|_\Gamma, \eta \right\rangle_{1/2} = \left\langle p^n_{nw,2}, \eta \right\rangle_\Gamma = 0$ for all $\eta \in H^{1/2}_{00}(\Gamma)$ and thus $p^n_{nw,2}\Big|_\Gamma = 0$.

Using this and integrating (21′) by parts yields $g_{nw,2} = \boldsymbol{F}^{\boldsymbol{n}}_{\boldsymbol{nw,2}} \cdot \boldsymbol{n_2}$. Since $g_{nw,2} = -g_{nw,1} = \boldsymbol{F}^{\boldsymbol{n}}_{\boldsymbol{nw,1}} \cdot \boldsymbol{n_2}$ by (23′) and (26), the continuity of the fluxes follows.

Consequently, we have proven the following.

Lemma 1 (Limit of the LDD-TP–R solver) *Let $n \in \mathbb{N}, n \geq 1$, be fixed, the tuple $\left(\left(p^{n-1}_{w,1}, p^{n-1}_{w,2}\right), p^{n-1}_{nw,2}\right) \in \mathcal{V} \times H^1_0(\Omega_2)$ be given and assume that functions $(p^n_{w,1}, p^n_{w,2}, p^n_{nw,2}) \in \mathcal{V}_1 \times \mathcal{V}_2 \times \mathcal{V}_2$ and $g_{\alpha,l} \in H^{1/2}_{00}(\Gamma)'$ exist for $\alpha \in \{n, nw\}$ and $l \in \{1,2\}$, such that $g_{nw,1}$ is given by (26), and such that these functions fulfill the system of equations (19′)-(23′) for all $\varphi_{w,1} \in \mathcal{V}_1$ and $\varphi_{w,2}, \varphi_{nw,2} \in \mathcal{V}_2$.*
Then, the interface conditions

$$p^n_{w,1}|_\Gamma = p^n_{w,2}|_\Gamma \quad \textit{and} \quad p^n_{nw,2}|_\Gamma = 0, \tag{27}$$

$$\boldsymbol{F}^{\boldsymbol{n}}_{\boldsymbol{\alpha,l}} \cdot \boldsymbol{n_l} = \boldsymbol{F}^{\boldsymbol{n}}_{\boldsymbol{\alpha,3-l}} \cdot \boldsymbol{n_l}, \quad \alpha \in \{w, nw\} \quad (l \in \{1,2\}) \tag{28}$$

are satisfied in $H^{1/2}_{00}(\Gamma)'$ and $\left(\left(p^n_{w,1}, p^n_{w,2}\right), p^n_{nw,2}\right)$ solves Problem 2. Moreover,

$$g_{w,l} = -\lambda_w p^n_{w,l}|_\Gamma + \boldsymbol{F}^{\boldsymbol{n}}_{\boldsymbol{w,l}} \cdot \boldsymbol{n_l} \quad (l = 1,2) \quad \textit{and} \tag{29}$$

$$g_{nw,2} = -\lambda_{nw} p^n_{nw,2}|_\Gamma + \boldsymbol{F}^{\boldsymbol{n}}_{\boldsymbol{nw,2}} \cdot \boldsymbol{n_2} \tag{30}$$

in $H^{1/2}_{00}(\Gamma)'$.

Conversely, if $\left(\left(p^n_{w,1},\, p^n_{w,2}\right), p^n_{nw,2}\right) \in \mathcal{V} \times H^1_0(\Omega_2)$ *is a solution of Problem 2 and* $g_{w,l}$ *is defined according to (29),* $g_{nw,2}$ *according to (30) and* $g_{nw,1}$ *given by (26), then* $\left(\left(p^n_{w,1}, p^n_{w,2}\right), p^n_{nw,2}\right)$ *and* $g_{\alpha,l}$ *solve the system* (19′)–(23′).

Remark 6 Theorem 1 below shows that the family $\left\{\left(p^{n,i}_{w,1}, p^{n,i}_{w,2}, p^{n,i}_{nw,2}\right)\right\}_{i\in\mathbb{N}}$ of subsequent solutions to Problem 3, together with the iterates $\left\{g^i_{\alpha,l}\right\}_{i\in\mathbb{N}}$ converge to a solution of (19′)–(23′). By the just proven lemma, this means solving Problem 2. Thus, it is justified to refer to equations (19′)–(23′) as the limit system to Problem 3.

3 | CONVERGENCE OF THE LDD-TP–R SOLVER

In this core section we analyze the convergence of the LDD-TP–R solver. Before doing so we state the general assumptions needed (see also the setting in [4, 37]).

Assumption 1 Let $l \in \{1,2\}$.
(a) The intrinsic permeabilities $k_{\mathrm{i},l}$ belong to $L^\infty(\Omega, \mathbb{R}_+) \cap C^{0,1}(\Omega, \mathbb{R}_+)$.
(b) The relative permeabilities of the wetting phases $k_{w,l} : [0,1] \to [0,1]$ are strictly monotonically increasing and Lipschitz continuous functions with Lipschitz constants $L_{k_{w,l}}$. The relative permeabilities of the nonwetting phases $k_{nw,l} : [0,1] \to [0,1]$ on both domains are strictly monotonically decreasing (as functions of the wetting saturation) and Lipschitz continuous functions with Lipschitz constants $L_{k_{nw,l}}$.
(c) There are numbers $m_1, m_2 > 0$ such that we have $\frac{k_{\mathrm{i},l} k_{w,1}}{\mu_w} \geq m_1$ and

$$m_2 = \min\left\{ \min_{s\in[0,1]} \frac{k_{\mathrm{i},2}}{\mu_w} k_{w,2}(s),\ \min_{s\in[0,1]} \frac{k_{\mathrm{i},2}}{\mu_{nw}} k_{nw,2}(s) \right\}. \tag{31}$$

(d) The capillary pressure saturation relationships $p^l_c(S_l) := p_{nw,l} - p_{w,l}$ are monotonically decreasing functions and therefore the saturations, $S_l\left(p^l_c\right) = S_l\left(p_{nw,l} - p_{w,l}\right)$ are also monotonically decreasing as functions of p^l_c. Moreover, they are assumed to be Lipschitz continuous with Lipschitz constants L_{S_l}.

Assumption 1(c) is required to ensure the existence of a solution in each LDD-TP–R solver step, and for the convergence proof of the LDD-TP–R solver as well. It excludes degeneracy and implicitly makes sure that both phases are present on both sides of the interface avoiding trapping effects.

Before stating our main result, we note the following lemma. In view of Assumption 1 it is a direct consequence of the Lax-Milgram theorem and guarantees that solving Problem 3 is always possible.

Lemma 3 *Let Assumptions 1 hold true. Given* $f^n_{\alpha,l} \in \mathcal{V}_{l'}$*, Problem 3 has a unique solution* $\left(p^{n,i}_{w,1}, p^{n,i}_{w,2}, p^{n,i}_{nw,2}\right) \in \mathcal{V}_1 \times \mathcal{V}_2 \times \mathcal{V}_2$.

Considering a family of subsequent solutions to Problem 3, we can now prove the following convergence result for the LDD-TP–R solver.

Theorem 1 (Convergence of the LDD-TP–R solver) *Let Assumption 1 hold true and suppose that there exists a pair* $\left(\left(p^n_{w,1}, p^n_{w,2}\right), p^n_{nw,2}\right) \in \mathcal{V} \times H^1_0(\Omega_2)$ *that uniquely solves Problem 2 satisfying for some* $M > 0$ *the bound* $\sup_{l,\alpha} \|\nabla\left(p^n_{\alpha,l} + z_\alpha\right)\|_{L^\infty} \leq M$*. For*

$l \in \{1,2\}, \alpha \in \{w, nw\}$ let $\lambda_\alpha > 0$ and $L_{\alpha,l} > 0$ be such that we have

$$\frac{1}{L_{S_2}\Phi_2} - \sum_\alpha \frac{1}{2L_{\alpha,2}} > 0 \quad \text{and} \quad \frac{1}{L_{S_1}\Phi_1} - \frac{1}{2L_{w,1}} > 0. \tag{32}$$

For arbitrary initial pressures $p_{w,l}^{n,0} := v_{w,l} \in \mathcal{V}_l$, $l = 1,2$, and $p_{nw,2}^{n,0} := v_{nw,2} \in H_0^1(\Omega_2)$, let $\left\{\left(\left(p_{w,1}^{n,i}, p_{w,2}^{n,i}\right), p_{nw,2}^{n,i}\right)\right\}_{i\in\mathbb{N}_0} \in (\mathcal{V}_1 \times \mathcal{V}_2 \times \mathcal{V}_2)^{\mathbb{N}_0}$ be a sequence of solutions to Problem 3, $\left\{g_{\alpha,l}^i\right\}_{i\in\mathbb{N}_0}$ be defined by (20) and (22)–(23) and $g_{\alpha,l}$ by (24)–(25) for $\alpha \in \{w, nw\}$ and $l \in \{1,2\}$. Assume, that the time step size τ has been chosen to satisfy the conditions

$$C_2 := \frac{1}{L_{S_2}\Phi_2} - \sum_\alpha \frac{1}{2L_{\alpha,2}} - \tau \sum_\alpha \frac{L_{k_{\alpha,2}}^2 M^2}{2m_2\Phi_2^2} > 0, \qquad C_1 := \frac{1}{L_{S_1}\Phi_1} - \frac{1}{2L_{w,1}} - \tau \frac{L_{k_{w,1}}^2 M^2}{2m_1\Phi_1^2} > 0. \tag{33}$$

Then,

$$\begin{array}{lll} p_{w,l}^{n,i} & \to p_{w,l}^n & \text{in } \mathcal{V}_l \\ p_{nw,2}^{n,i} & \to p_{nw,2}^n & \text{in } \mathcal{V}_2 \end{array}, \quad \text{and} \quad \begin{array}{lll} g_{w,l}^i & \to g_{w,l} & \text{in } \mathcal{V}_{l'} \\ g_{nw,l}^i & \to g_{nw,l} & \text{in } \mathcal{V}_{l'} \end{array},$$

for $l = 1,2$ as $i \to \infty$. Notably, $p_{nw,2}^{n,i}\big|_\Gamma \to 0$ in $H_{00}^{1/2}(\Gamma)$ as $i \to \infty$.

Remark 7 (Explicit time step restriction) The implicit restrictions (33) on the time step size translate to the explicit form

$$\tau < \min\left\{\left(\frac{1}{L_{S_1}\Phi_1} - \frac{1}{2L_{w,1}}\right)\frac{2m_1\Phi_1^2}{L_{k_{w,1}}^2 M^2}, \frac{\frac{1}{L_{S_2}\Phi_2} - \sum_\alpha \frac{1}{2L_{\alpha,2}}}{\sum_\alpha \left[\left(L_{k_{\alpha,2}}M\right)^2 / \left(2m_2\Phi_2^2\right)\right]}\right\}. \tag{34}$$

The above time step restriction is an assumption necessary for our convergence proof to work. It is in no shape or form a sharp estimate. For practical numerical application the value of τ must be guessed. It needs to be balanced between assuring convergence of the scheme and reasonable simulation time. It is a general trait of L-type schemes, however, to issue stable convergence behavior with coarser time step sizes, compare [1]. We test this numerically in paragraph 5.1, see p. 20.

Proof. (of Theorem 3.3)**.** Note that for the proof, we will actually denote by $L_{k_{\alpha,l}}$ the Lipschitz constant of the function $\frac{\|k_{i,l}\|_\infty k_{\alpha,l}}{\mu_\alpha}$ by slight abuse of notation. Define the iteration errors $e_{p,l}^{w,i} := p_{w,l}^n - p_{w,l}^{n,i}$ and $e_{p,2}^{nw,i} := p_{nw,2}^n - p_{nw,2}^{n,i}$ as well as $e_{g,l}^{\alpha,i} := g_{\alpha,l} - g_{\alpha,l}^i$ for $l = 1,2$ and $\alpha \in \{w, nw\}$. Add $L_{w,l}\left\langle p_{w,l}^n, \varphi_{w,l}\right\rangle - L_{w,l}\left\langle p_{w,l}^n, \varphi_{w,l}\right\rangle$ to (19) and respectively $L_{nw,2}\left\langle p_{nw,2}^n, \varphi_{nw,2}\right\rangle - L_{nw,2}\left\langle p_{nw,2}^n, \varphi_{nw,2}\right\rangle$ to (21) and subtract the corresponding equations (19) as well as (21) to get

$$\begin{aligned} &L_{\alpha,l}\left\langle e_{p,l}^{\alpha,i} - e_{p,l}^{\alpha,i-1}, \varphi_{\alpha,l}\right\rangle + \tau\left\langle \lambda_\alpha e_{p,l}^{\alpha,i} + e_{g,l}^{\alpha,i}, \varphi_{\alpha,l}\right\rangle_\Gamma \\ &+\tau\left\langle -\boldsymbol{F}_{\alpha,l}^{n} - k_{\alpha,l}^{n,i-1}\nabla\left(p_{\alpha,l}^n + z_\alpha\right) + k_{\alpha,l}^{n,i-1}\nabla\left(p_{\alpha,l}^n + z_\alpha\right) + \boldsymbol{F}_{\alpha,l}^{n,i}, \nabla\varphi_{\alpha,l}\right\rangle \\ &= \underbrace{(-1)^{\delta_{\alpha w}}\left\langle \Phi_l S_l^n - \Phi_l S_l^{n-1}, \varphi_{\alpha,l}\right\rangle - (-1)^{\delta_{\alpha w}}\left\langle \Phi_l S_l^{n,i-1} - \Phi_l S_l^{n-1}, \varphi_{\alpha,l}\right\rangle}_{(-1)^{\delta_{\alpha w}}\left\langle \Phi_l S_l^n - \Phi_l S_l^{n,i-1}, \varphi_{\alpha,l}\right\rangle}, \end{aligned} \tag{35}$$

where (35) is meaningful for the index combinations $(\alpha, l) \in \{(w,1),(w,2),(nw,2)\}$. Note the use of the Kronecker delta $\delta_{\alpha w}$ to account for the minus sign of the time discretization for the nonwetting phase.

Inserting for all admissible index combinations $\varphi_{\alpha,l} := e_{p,l}^{\alpha,i}$ in (35) and making use of the identity

$$L_{\alpha,l}\left\langle e_{p,l}^{\alpha,i}-e_{p,l}^{\alpha,i-1}, e_{p,l}^{\alpha,i}\right\rangle = \frac{L_{\alpha,l}}{2}\left(\|e_{p,l}^{\alpha,i}\|^2-\|e_{p,l}^{\alpha,i-1}\|^2+\|e_{p,l}^{\alpha,i}-e_{p,l}^{\alpha,i-1}\|^2\right),$$

leads to

$$\frac{L_{\alpha,l}}{2}\left(\|e_{p,l}^{\alpha,i}\|^2-\|e_{p,l}^{\alpha,i-1}\|^2+\|e_{p,l}^{\alpha,i}-e_{p,l}^{\alpha,i-1}\|^2\right)+\tau\lambda_\alpha\left\langle e_{p,l}^{\alpha,i}, e_{p,l}^{\alpha,i}\right\rangle_\Gamma = \left\langle \Phi_l S_l^n-\Phi_l S_l^{n,i-1}, (-1)^{\delta_{\alpha w}} e_{p,l}^{\alpha,i}\right\rangle$$
$$-\tau\left\langle e_{g,l}^{\alpha,i}, e_{p,l}^{\alpha,i}\right\rangle_\Gamma-\tau\left\langle\left(k_{\alpha,l}^n-k_{\alpha,l}^{n,i-1}\right)\nabla\left(p_{\alpha,l}^n+z_\alpha\right), \nabla e_{p,l}^{\alpha,i}\right\rangle-\tau\left\langle k_{\alpha,l}^{n,i-1}\nabla e_{p,l}^{\alpha,i}, \nabla e_{p,l}^{\alpha,i}\right\rangle. \tag{36}$$

Summing over phases $\alpha = w, nw$ in (36) for $l = 2$ and adding the term $\left\langle \Phi_2 S_2^n-\Phi_2 S_2^{n,i-1}, e_{p,2}^{w,i-1}-e_{p,2}^{nw,i-1}\right\rangle$ on both sides of the equation, yields

$$\sum_\alpha \frac{L_{\alpha,2}}{2}\left(\|e_{p,2}^{\alpha,i}\|^2-\|e_{p,2}^{\alpha,i-1}\|^2+\|e_{p,2}^{\alpha,i}-e_{p,2}^{\alpha,i-1}\|^2\right)+\underbrace{\left\langle \Phi_2 S_2^n-\Phi_2 S_2^{n,i-1}, e_{p,2}^{w,i-1}-e_{p,2}^{nw,i-1}\right\rangle}_{TP_1}$$
$$=\underbrace{\left\langle \Phi_2 S_2^n-\Phi_2 S_2^{n,i-1}, e_{p,2}^{w,i-1}-e_{p,2}^{w,i}-\left(e_{p,2}^{nw,i-1}-e_{p,2}^{nw,i}\right)\right\rangle}_{=:TP_2}-\tau\underbrace{\sum_\alpha\left\langle \lambda_\alpha e_{p,2}^{\alpha,i}+e_{g,2}^{\alpha,i}, e_{p,2}^{\alpha,i}\right\rangle_\Gamma}_{=:I_{TP}}$$
$$-\tau\underbrace{\sum_\alpha\left\langle k_{\alpha,2}^{n,i-1}\nabla e_{p,2}^{\alpha,i}, \nabla e_{p,2}^{\alpha,i}\right\rangle}_{=:TP_4}-\tau\underbrace{\sum_\alpha\left\langle\left(k_{\alpha,2}^n-k_{\alpha,2}^{n,i-1}\right)\nabla\left(p_{\alpha,2}^n+z_\alpha\right), \nabla e_{p,2}^{\alpha,i}\right\rangle}_{=:TP_3}. \tag{37}$$

Similarly, adding $\left\langle \Phi_1 S_1^n-\Phi_1 S_1^{n,i-1}, e_{p,1}^{w,i-1}\right\rangle$ to both sides of (36) for $l = 1$, one gets

$$\frac{L_{w,1}}{2}\left(\|e_{p,1}^{w,i}\|^2-\|e_{p,1}^{w,i-1}\|^2+\|e_{p,1}^{w,i}-e_{p,1}^{w,i-1}\|^2\right)+\underbrace{\left\langle \Phi_1 S_1^n-\Phi_1 S_1^{n,i-1}, e_{p,1}^{w,i-1}\right\rangle}_{R_1}$$
$$=\underbrace{\left\langle \Phi_1 S_1^n-\Phi_1 S_1^{n,i-1}, e_{p,1}^{w,i-1}-e_{p,1}^{w,i}\right\rangle}_{=:R_2}-\tau\underbrace{\left\langle \lambda_w e_{p,1}^{w,i}+e_{g,1}^{w,i}, e_{p,1}^{w,i}\right\rangle_\Gamma}_{=:I_R}$$
$$-\underbrace{\tau\left\langle\left(k_{w,1}^n-k_{w,1}^{n,i-1}\right)\nabla\left(p_{w,1}^n+z_w\right), \nabla e_{p,1}^{w,i}\right\rangle}_{=:R_3}-\underbrace{\tau\left\langle k_{w,1}^{n,i-1}\nabla e_{p,1}^{w,i}, \nabla e_{p,1}^{w,i}\right\rangle}_{=:R_4}. \tag{38}$$

We proceed to estimate the assigned terms TP_1–TP_4 and R_1–R_4 from (37) and (38).

TP_1, R_1 Recall that $S_l\left(p_{w,l}, p_{nw,l}\right) = \left(p_c^l\right)^{-1}\left(p_{nw,l}-p_{w,l}\right)$ for both l and that $p_c^{l\,\prime} < 0$ so that we actually have the dependence $S_l\left(p_{w,l}, p_{nw,l}\right) = S_l\left(p_{nw,l}-p_{w,l}\right)$ where S_l as a function of p_c^l is monotonically decreasing. Even though $p_{nw,1} = p_a = 0$ and there is no equation for $p_{nw,1}$, we estimate both TP_1 and R_1 with the same reasoning by setting $p^n_{nw,1} = 0$ and $p^{n,i}_{nw,1} = 0$ for all $i \in \mathbb{N}$. Thereby, we have *for* $l = 1, 2$

$$\left|\Phi_l S_l \left(p^n_{nw,l} - p^n_{w,l}\right) - \Phi_l S_l \left(p^{n,i-1}_{nw,l} - p^{n,i-1}_{w,l}\right)\right|^2$$

$$\leq L_{S_l}\Phi_l|\Phi_l S_l \left(p^n_{nw,l} - p^n_{w,l}\right) - \Phi_l S_l \left(p^{n,i-1}_{nw,l} - p^{n,i-1}_{w,l}\right)||e^{nw,i-1}_{p,l} - e^{w,i-1}_{p,l}|$$

$$= L_{S_l}\Phi_l \left(\Phi_l S_l \left(p^n_{nw,l} - p^n_{w,l}\right) - \Phi_l S_l \left(p^{n,i-1}_{nw,l} - p^{n,i-1}_{w,l}\right)\right)\left(e^{w,i-1}_{p,l} - e^{nw,i-1}_{p,l}\right) \tag{39}$$

as a result of the Lipschitz continuity of S_l. The monotonicity of S_l allowed dropping the absolute value. Therefore, by integrating (39), we estimate TP_1 and R_1 by

$$\frac{1}{L_{S_l}\Phi_l}\|\Phi_l S^n_l - \Phi_l S^{n,i-1}_l\|^2 \leq \left\langle \Phi_l S^n_l - \Phi_l S^{n,i-1}_l, e^{w,i-1}_{p,l} - e^{nw,i-1}_{p,l}\right\rangle. \tag{40}$$

For $l = 1$, (40) is an estimate for R_1 since we had set $e^{nw,i-1}_{p,1} = 0$, and for $l = 2$ it is an estimate for TP_1. In this manner, (40) is a condensed notation of both estimates into one.

TP_2, R_2 Young's inequality $|xy| \leq \varepsilon|x|^2 + \frac{1}{4\varepsilon}|y|^2$ with $\varepsilon > 0$ applied to the term TP_2, gives

$$|TP_2| = |\left\langle \Phi_2 S^n_2 - \Phi_2 S^{n,i-1}_2, e^{w,i-1}_{p,2} - e^{w,i}_{p,2} - \left(e^{nw,i-1}_{p,2} - e^{nw,i}_{p,2}\right)\right\rangle| \leq \frac{L_{w,2}}{2}\|e^{w,i-1}_{p,2} - e^{w,i}_{p,2}\|^2$$

$$+\frac{L_{nw,2}}{2}\left\|\left(e^{nw,i-1}_{p,2} - e^{nw,i}_{p,2}\right)\right\|^2 + \left(\frac{1}{2L_{w,2}} + \frac{1}{2L_{nw,2}}\right)\|\Phi_2 S^n_2 - \Phi_2 S^{n,i-1}_2\|^2,$$

where we chose $\varepsilon^2_\alpha = \frac{L_{\alpha,2}}{2}$ for $\alpha = w, nw$. The analogous choice of $\varepsilon^1_w = \frac{L_{w,1}}{2}$ for $l = 1$ yields

$$|R_2| = |\left\langle \Phi_1 S^n_1 - \Phi_1 S^{n,i-1}_1, e^{w,i-1}_{p,1} - e^{w,i}_{p,1}\right\rangle| \leq \frac{L_{w,1}}{2}\|e^{w,i-1}_{p,1} - e^{w,i}_{p,1}\|^2 + \frac{1}{2L_{w,1}}\|\Phi_1 S^n_1 - \Phi_1 S^{n,i-1}_1\|^2.$$

TP_3, R_3. TP_3 and R_3 can be estimated together as well. We have

$$|\left\langle\left(k^n_{\alpha,l} - k^{n,i-1}_{\alpha,l}\right)\nabla\left(p^n_{\alpha,l} + z_\alpha\right), \nabla e^{\alpha,i}_{p,l}\right\rangle| \leq \left\|\left(k^n_{\alpha,l} - k^{n,i-1}_{\alpha,l}\right)\nabla\left(p^n_{\alpha,l} + z_\alpha\right)\right\|\|\nabla e^{\alpha,i}_{p,l}\|$$

$$\leq \frac{L_{k_{\alpha,l}}M}{\Phi_l}\|\Phi_l S^n_l - \Phi_l S^{n,i}_l\|\|\nabla e^{\alpha,i}_{p,l}\| \leq \frac{L_{k_{\alpha,l}}M}{\Phi_l}\varepsilon_{\alpha,l}\|\Phi_l S^n_l - \Phi_l S^{n,i}_l\|^2 + \frac{L_{k_{\alpha,l}}M}{4\varepsilon_{\alpha,l}\Phi_l}\|\nabla e^{\alpha,i}_{p,l}\|^2 \tag{41}$$

for $(\alpha, l) \in \{(w, 1), (w, 2), (nw, 2)\}$. To derive (41), the Lipschitz-continuity of $k_{\alpha,l}$ and the assumption $\|\nabla\left(p^n_{\alpha,l} + z_\alpha\right)\|_\infty < M$ was used. $\varepsilon_{\alpha,l}$ will be chosen later. Equation (41) is the estimate for R_3 for $l = 1, \alpha = w$ and the estimate for TP_3 is obtained by summing over the phase index α,

$$|TP_3| \leq \tau\sum_\alpha L_{k_{\alpha,2}}\frac{M\varepsilon_{\alpha,2}}{\Phi_2}\|\Phi_2 S^n_2 - \Phi_2 S^{n,i}_2\|^2 + \tau\sum_\alpha \frac{L_{k_{\alpha,2}}M}{4\varepsilon_{\alpha,2}\Phi_2}\|\nabla e^{\alpha,i}_{p,2}\|^2. \tag{42}$$

TP_4, R_4. Finally, by Assumption 1(c), we estimate R_4 by

$$R_4 = \tau\left\langle k^{n,i-1}_{w,1}\nabla e^{w,i}_{p,1}, \nabla e^{w,i}_{p,1}\right\rangle > \tau m_1\|\nabla e^{w,i}_{p,1}\|^2 \tag{43}$$

Analogously on the two-phase domain for TP_4, we have the estimate

$$TP_4 = \tau \sum_\alpha \left\langle k_{\alpha,2}^{n,i-1} \nabla e_{p,2}^{\alpha,i}, \nabla e_{p,2}^{\alpha,i} \right\rangle > \tau m_2 \sum_\alpha \|\nabla e_{p,2}^{\alpha,i}\|^2. \tag{44}$$

Combining the just derived estimates in (40)–(43) and (44) with Equations (37) and (38), one arrives at

$$\begin{aligned}
&\sum_\alpha \frac{L_{\alpha,2}}{2} \left(\|e_{p,2}^{\alpha,i}\|^2 - \|e_{p,2}^{\alpha,i-1}\|^2 \right) + \frac{1}{L_{S_2}\Phi_2} \|\Phi_2 S_2^n - \Phi_2 S_2^{n,i-1}\|^2 \\
&+\tau \sum_\alpha \left\langle \lambda_\alpha e_{p,2}^{\alpha,i} + e_{g,2}^{\alpha,i}, e_{p,2}^{\alpha,i} \right\rangle_\Gamma + \tau m_2 \sum_\alpha \|\nabla e_{p,2}^{\alpha,i}\|^2 \leq \sum_\alpha \frac{1}{2L_{\alpha,2}} \|\Phi_2 S_2^n - \Phi_2 S_2^{n,i-1}\|^2 \\
&+\tau \sum_\alpha \frac{L_{k_{\alpha,2}} M}{4\varepsilon_{\alpha,2}\Phi_2} \|\nabla e_{p,2}^{\alpha,i}\|^2 + \tau \sum_\alpha L_{k_{\alpha,2}} \frac{M\varepsilon_{\alpha,2}}{\Phi_2} \|\Phi_2 S_2^n - \Phi_2 S_2^{n,i}\|^2
\end{aligned} \tag{45}$$

on Ω_2, and on Ω_1 at

$$\begin{aligned}
&\frac{L_{w,1}}{2} \left(\|e_{p,1}^{w,i}\|^2 - \|e_{p,1}^{w,i-1}\|^2 \right) + \frac{1}{L_{S_1}\Phi_1} \|\Phi_1 S_1^n - \Phi_1 S_1^{n,i-1}\|^2 + \tau \left\langle \lambda_w e_{p,1}^{w,i} + e_{g,1}^{w,i}, e_{p,1}^{w,i} \right\rangle_\Gamma + \tau m_1 \|\nabla e_{p,1}^{w,i}\|^2 \\
&\leq \frac{1}{2L_{w,1}} \|\Phi_1 S_1^n - \Phi_1 S_1^{n,i-1}\|^2 + \tau \frac{L_{k_{\alpha,1}} M}{4\varepsilon_{w,1}\Phi_1} \|\nabla e_{p,1}^{w,i}\|^2 + \tau L_{k_{w,1}} \frac{M\varepsilon_{w,1}}{\Phi_1} \|\Phi_1 S_1^n - \Phi_1 S_1^{n,i}\|^2.
\end{aligned} \tag{46}$$

In order to handle the interface terms I_R in (38) and I_{TP} in (37), recall that we defined the pressure functionals according to Note 1. This allows us to treat the interface terms in the following way: Subtracting (20) from (20′) for $\alpha = w$ and (22), (23) from (22′) and (22), (23′) respectively for $\alpha = nw$, all the while using the representations $\overline{e_{g,l}^{\alpha,i}} \in H_{00}^{1/2}(\Gamma)$ of the functionals $e_{g,l}^{\alpha,i} \in H_{00}^{1/2}(\Gamma)'$(cf. Remark 2), we obtain

$$\overline{e_{g,l}^{\alpha,i}} = -2\lambda_\alpha e_{p,3-l}^{\alpha,i-1} - \overline{e_{g,3-l}^{\alpha,i-1}}$$

for $(\alpha, l) \in \{(w,1),(w,2),(nw,1)\}$ as well as

$$\overline{e_{g,2}^{nw,i}} = -\overline{e_{g,1}^{nw,i-1}}.$$

This leads to the relations

$$\|e_{p,l}^{w,i}\|_{1/2}^2 = \frac{1}{4\lambda_w^2} \left(\|\overline{e_{g,3-l}^{w,i+1}}\|_{1/2}^2 - \|\overline{e_{g,l}^{w,i}}\|_{1/2}^2 - 4\lambda_w \left\langle e_{g,l}^{w,i}, e_{p,l}^{w,i} \right\rangle_\Gamma \right), \tag{47}$$

$$\|e_{p,2}^{nw,i}\|_{1/2}^2 = \frac{1}{4\lambda_{nw}^2} \left(\|\overline{e_{g,1}^{nw,i+1}}\|_{1/2}^2 - \|\overline{e_{g,2}^{nw,i}}\|_{1/2}^2 - 4\lambda_{nw} \left\langle e_{g,2}^{nw,i}, e_{p,2}^{nw,i} \right\rangle_\Gamma \right), \tag{48}$$

$$0 = \frac{1}{4\lambda_{nw}^2} \left(\|\overline{e_{g,2}^{nw,i+1}}\|_{1/2}^2 - \|\overline{e_{g,1}^{nw,i}}\|_{1/2}^2 \right). \tag{49}$$

Inserting for $l = 1$ Equation (47) into (46) and for $l = 2$ (47) as well as (48) in (45), yields

$$\begin{aligned}
&\left(\frac{1}{L_{S_2}\Phi_2} - \sum_\alpha \left(\frac{1}{2L_{\alpha,2}} + \tau L_{k_{\alpha,2}} \frac{M\varepsilon_{\alpha,2}}{\Phi_2} \right) \right) \|\Phi_2 S_2^n - \Phi_2 S_2^{n,i-1}\|^2 + \tau \sum_\alpha \left(m_2 - \frac{L_{k_{\alpha,2}} M}{4\varepsilon_{\alpha,2}\Phi_2} \right) \|\nabla e_{p,2}^{\alpha,i}\|^2 \\
&\leq \sum_\alpha \frac{L_{\alpha,2}}{2} \left(\|e_{p,2}^{\alpha,i-1}\|^2 - \|e_{p,2}^{\alpha,i}\|^2 \right) + \tau \sum_\alpha \frac{1}{4\lambda_\alpha} \left(\|e_{g,2}^{\alpha,i}\|_{1/2}^2 - \|e_{g,1}^{\alpha,i+1}\|_{1/2}^2 \right)
\end{aligned} \tag{50}$$

for Ω_2 and

$$\left(\frac{1}{L_{S_1}\Phi_1}-\frac{1}{2L_{w,1}}-\tau L_{k_{w,1}}\frac{M\varepsilon_{w,1}}{\Phi_1}\right)\|\Phi_1 S_1^n-\Phi_1 S_1^{n,i-1}\|^2+\tau\left(m_1-\frac{L_{k_{w,1}}M}{4\varepsilon_{w,1}\Phi_1}\right)\|\nabla e_{p,1}^{w,i}\|^2$$

$$\leq \frac{L_{w,1}}{2}\left(\|e_{p,1}^{w,i-1}\|^2-\|e_{p,1}^{w,i}\|^2\right)+\frac{\tau}{4\lambda_w}\left(\|e_{g,1}^{w,i}\|_{1/2}^2-\|e_{g,2}^{w,i+1}\|_{1/2}^2\right), \tag{51}$$

for Ω_1, where we dropped denoting the representing element by $\bar{\cdot}$.

Now choose $\varepsilon_{\alpha,l}=L_{k_{\alpha,l}}M/(2m_l\Phi_l)$ such that $m_l-L_{k_{\alpha,l}}M/\left(4\varepsilon_{\alpha,l}\Phi_l\right)=\frac{m_l}{2}>0$. Recall that by assumption the numbers $L_{\alpha,l}$ have been chosen large enough that $\frac{1}{L_{S_2}\Phi_2}-\frac{1}{2}\sum_\alpha\frac{1}{L_{\alpha,2}}>0$ as well as $\frac{1}{L_{S_1}\Phi_1}-\frac{1}{2L_{w,1}}>0$, and in addition the time step restriction (33) is satisfied for a sufficiently small τ. Summing up the equations (50) and (51), then adding zero in the form of (49) to the result and thereafter summing with respect to iterations $i=1,\ldots,r$ leads to

$$\sum_{i=1}^{r}\sum_{l=1,2}C_l\|\Phi_l S_l^n-\Phi_l S_l^{n,i-1}\|^2+\tau\sum_{i=1}^{r}\left(\frac{m_1}{2}\|\nabla e_{p,1}^{w,i}\|^2+\frac{m_2}{2}\sum_\alpha\|\nabla e_{p,2}^{\alpha,i}\|^2\right)$$

$$\leq\sum_\alpha\frac{L_{\alpha,2}}{2}\left(\|e_{p,2}^{\alpha,0}\|^2-\|e_{p,2}^{\alpha,r}\|^2\right)+\frac{L_{w,1}}{2}\left(\|e_{p,1}^{w,0}\|^2-\|e_{p,1}^{w,r}\|^2\right)$$

$$+\tau\sum_{l=1}^{2}\sum_\alpha\frac{1}{4\lambda_\alpha}\left(\|e_{g,l}^{\alpha,1}\|_{1/2}^2-\|e_{g,l}^{\alpha,r+1}\|_{1/2}^2\right), \tag{52}$$

where C_l is defined in (33) and the telescopic nature of the sums on the right hand side have been exploited. Equation (52) implies the estimates

$$\sum_{i=1}^{r}\sum_{l=1}^{2}C_l\|\Phi_l S_l^n-\Phi_l S_l^{n,i-1}\|^2\leq C, \tag{53}$$

$$\tau\sum_{i=1}^{r}\left(\frac{m_1}{2}\|\nabla e_{p,1}^{w,i}\|^2+\frac{m_2}{2}\sum_\alpha\|\nabla e_{p,2}^{\alpha,i}\|^2\right)\leq C, \tag{54}$$

$$\sum_\alpha\frac{L_{\alpha,2}}{2}\|e_{p,2}^{\alpha,r}\|^2+\frac{L_{w,1}}{2}\|e_{p,1}^{w,r}\|^2+\tau\sum_{l=1}^{2}\sum_\alpha\frac{1}{4\lambda_\alpha}\|e_{g,l}^{\alpha,r+1}\|_{1/2}^2\leq C, \tag{55}$$

with

$$C:=\sum_\alpha\frac{L_{\alpha,2}}{2}\|e_{p,2}^{\alpha,0}\|^2+\frac{L_{w,1}}{2}\|e_{p,1}^{w,0}\|^2+\tau\sum_{l=1}^{2}\sum_\alpha\frac{1}{4\lambda_\alpha}\|e_{g,l}^{\alpha,1}\|_{1/2}^2.$$

Since C is independent of r, we thereby conclude that

$$\|\Phi_l S_l^n-\Phi_l S_l^{n,i-1}\|,\ \|\nabla e_{p,l}^{\alpha,i}\|\to 0\quad\text{as}\quad i\to\infty, \tag{56}$$

for all appearing combinations of $l\in\{1,2\}$ and $\alpha\in\{w,nw\}$. Due to the partial homogeneous Dirichlet boundary, the Poincaré inequality is applicable compare [32, Theorem A.2.5, p. 252] for functions in $\mathcal{V}_l$. Thus, equation (56) further implies $\|e_{p,l}^{\alpha,i}\|\to 0$ as $i\to\infty$ for all admissible index combinations.

In order to show that $e^{\alpha,i}_{g,l} \to 0$ in $\mathcal{V}_{l'}$ for all appearing indices, we subtract (19) from (19′) for $\alpha = w$, $l = 1, 2$, and (21) from (21′) for $\alpha = nw$, $l = 2$ and consider only test functions in $\varphi_{\alpha,l} \in C_0^\infty(\Omega_l)$, that is,

$$-\tau\left\langle \boldsymbol{F}^{\boldsymbol{n}}_{\boldsymbol{\alpha},\boldsymbol{l}} - \boldsymbol{F}^{\boldsymbol{n},\boldsymbol{i}}_{\boldsymbol{\alpha},\boldsymbol{l}}, \nabla\varphi_{\alpha,l}\right\rangle = L_{\alpha,l}\left\langle e^{\alpha,i-1}_{p,l} - e^{\alpha,i}_{p,l}, \varphi_{\alpha,l}\right\rangle + (-1)^{\delta_{\alpha w}}\left\langle \Phi_l S^n_l - \Phi_l S^{n,i-1}_l, \varphi_{\alpha,l}\right\rangle. \tag{57}$$

Thus, $\nabla\cdot\left(\boldsymbol{F}^{\boldsymbol{n}}_{\boldsymbol{\alpha},\boldsymbol{l}} - \boldsymbol{F}^{\boldsymbol{n},\boldsymbol{i}}_{\boldsymbol{\alpha},\boldsymbol{l}}\right)$ exists in $L^2(\Omega_l)$ and

$$-\tau\nabla\cdot\left(\boldsymbol{F}^{\boldsymbol{n}}_{\boldsymbol{\alpha},\boldsymbol{l}} - \boldsymbol{F}^{\boldsymbol{n},\boldsymbol{i}}_{\boldsymbol{\alpha},\boldsymbol{l}}\right) = L_{\alpha,l}\left(e^{\alpha,i}_{p,l} - e^{\alpha,i-1}_{p,l}\right) + (-1)^{\delta_{\alpha nw}}\left(\Phi_l S^n_l - \Phi_l S^{n,i-1}_l\right) \tag{58}$$

almost everywhere, from which we deduce for $\varphi_{\alpha,l}$ now taken to be in $\mathcal{V}_l$

$$\left|\left\langle \nabla\cdot\left(\boldsymbol{F}^{\boldsymbol{n}}_{\boldsymbol{\alpha},\boldsymbol{l}} - \boldsymbol{F}^{\boldsymbol{n},\boldsymbol{i}}_{\boldsymbol{\alpha},\boldsymbol{l}}\right), \varphi_{\alpha,l}\right\rangle\right| \leq \frac{L_{\alpha,l}}{\tau}\|e^{\alpha,i}_{p,l} - e^{\alpha,i-1}_{p,l}\|\|\varphi_{\alpha,l}\| + \frac{1}{\tau}\|\Phi_l S^n_l - \Phi_l S^{n,i-1}_l\|\|\varphi_{\alpha,l}\|. \tag{59}$$

Introducing the abbreviation $|\Psi^{n,i}_{\alpha,l}(\varphi_{\alpha,l})|$ for the left hand side of (59), the limit

$$\sup_{\substack{\varphi_{\alpha,l}\in\mathcal{V}_l\\ \varphi_{\alpha,l}\neq 0}} \frac{|\Psi^{n,i}_{\alpha,l}(\varphi_{\alpha,l})|}{\|\varphi_{\alpha,l}\|_{\mathcal{V}_l}} \leq \frac{L_{\alpha,l}}{\tau}\left\|e^{\alpha,i}_{p,l} - e^{\alpha,i-1}_{p,l}\right\| + \frac{1}{\tau}\left\|\Phi_l S^n_l - \Phi_l S^{n,i-1}_l\right\| \to 0$$

as $i \to \infty$ follows as a consequence of (53) and (54). In other words $\|\Psi^{n,i}_{\alpha,l}\|_{\mathcal{V}_{l'}} \to 0$ as $i \to \infty$. On the other hand, starting again from (35) (without the added zero term), this time however inserting $\varphi_{\alpha,l} \in \mathcal{V}_l$ and integrating by parts, keeping in mind (58), one deduces that

$$\left\langle e^{\alpha,i}_{g,l}, \varphi_{\alpha,l}\right\rangle_\Gamma = -\lambda_\alpha\left\langle e^{\alpha,i}_{p,l}, \varphi_{\alpha,l}\right\rangle_\Gamma + \left\langle\left(\boldsymbol{F}^{\boldsymbol{n}}_{\boldsymbol{\alpha},\boldsymbol{l}} - \boldsymbol{F}^{\boldsymbol{n},\boldsymbol{i}}_{\boldsymbol{\alpha},\boldsymbol{l}}\right)\cdot\boldsymbol{n}_{\boldsymbol{l}}, \varphi_{\alpha,l}\right\rangle_\Gamma. \tag{60}$$

We already know, that $\|e^{\alpha,i}_{p,l}\|_{\mathcal{V}_l} \to 0$ as $i \to 0$ and we will use the continuity of the trace operator to deal with the term $\left\langle e^{\alpha,i}_{p,l}, \varphi_{\alpha,l}\right\rangle_\Gamma$. For the last summand in (60) we have by the integration by parts formula

$$\left\langle\left(\boldsymbol{F}^{\boldsymbol{n}}_{\boldsymbol{\alpha},\boldsymbol{l}} - \boldsymbol{F}^{\boldsymbol{n},\boldsymbol{i}}_{\boldsymbol{\alpha},\boldsymbol{l}}\right)\cdot\boldsymbol{n}_{\boldsymbol{l}}, \varphi_{\alpha,l}\right\rangle_\Gamma = \Psi^{n,i}_{\alpha,l}(\varphi_{\alpha,l}) + \left\langle \boldsymbol{F}^{\boldsymbol{n}}_{\boldsymbol{\alpha},\boldsymbol{l}} - \boldsymbol{F}^{\boldsymbol{n},\boldsymbol{i}}_{\boldsymbol{\alpha},\boldsymbol{l}}, \nabla\varphi_{\alpha,l}\right\rangle, \tag{61}$$

and the second term can be estimated by

$$\begin{aligned}
&\left|\left\langle k^n_{\alpha,l}\nabla\left(p^n_{\alpha,l} + z_\alpha\right) - k^{n,i-1}_{\alpha,l}\nabla\left(p^{n,i}_{\alpha,l} + z_\alpha\right), \nabla\varphi_{\alpha,l}\right\rangle\right| \\
&\leq \left|\left\langle\left(k^n_{\alpha,l} - k^{n,i-1}_{\alpha,l}\right)\nabla\left(p^n_{\alpha,l} + z_\alpha\right) - k^{n,i-1}_{\alpha,l}\nabla e^{\alpha,i}_{p,l}, \nabla\varphi_{\alpha,l}\right\rangle\right| \\
&\leq \frac{L_{k_{\alpha,l}}M}{\Phi_l}\left\|\Phi_l S^n_l - \Phi_l S^{n,i-1}_l\right\|\left\|\varphi_{\alpha,l}\right\|_{\mathcal{V}_l} + M_{k_{\alpha,l}}\left\|\nabla e^{\alpha,i}_{p,l}\right\|\left\|\varphi_{\alpha,l}\right\|_{\mathcal{V}_l},
\end{aligned}$$

where we used the same reasoning as in (41) and $\max|k_{\alpha,l}| \leq M_{k_{\alpha,l}}$. With this, we get

$$\sup_{\substack{\varphi_{\alpha,l}\in\mathcal{V}_l\\ \|\varphi_{\alpha,l}\|_{\mathcal{V}_l}=1}} \left|\left\langle\left(\boldsymbol{F}^{\boldsymbol{n}}_{\boldsymbol{\alpha},\boldsymbol{l}} - \boldsymbol{F}^{\boldsymbol{n},\boldsymbol{i}}_{\boldsymbol{\alpha},\boldsymbol{l}}\right)\cdot\boldsymbol{n}_{\boldsymbol{l}}, \varphi_{\alpha,l}\right\rangle_\Gamma\right| \leq \left\|\Psi^{n,i}_{\alpha,l}\right\|_{\mathcal{V}_{l'}} + \frac{L_{k_{\alpha,l}}M}{\Phi_l}\left\|\Phi_l S^n_l - \Phi_l S^{n,i-1}_l\right\| + M_{k_{\alpha,l}}\left\|\nabla e^{\alpha,i}_{p,l}\right\| \to 0,$$

as $i \to \infty$ from (61). Finally, we deduce from (60) and the continuity of the trace operator (with constant $\widetilde{C}$) on Lipschitz domains

$$\sup_{\substack{\varphi_{\alpha,l}\in\mathcal{V}_l\\ \varphi_{\alpha,l}\neq 0}} \frac{\left|\left\langle e_{g,l}^{\alpha,i}, \varphi_{\alpha,l}\right\rangle_\Gamma\right|}{\left\|\varphi_{\alpha,l}\right\|_{\mathcal{V}_l}} \le \lambda_\alpha \widetilde{C}\left\|e_{p,l}^{\alpha,i}\right\|_{\mathcal{V}_l} + \left\|\Psi_{\alpha,l}^{n,i}\right\|_{\mathcal{V}_{l'}} + \frac{L_{k_{\alpha,l}}M}{\Phi_l}\left\|\Phi_l S_l^n - \Phi_l S_l^{n,i-1}\right\| + M_{k_{\alpha,l}}\left\|\nabla e_{p,l}^{\alpha,i}\right\| \to 0,$$

as $i \to \infty$. This shows $e_{g,l}^{\alpha,i} \to 0$ in $\mathcal{V}_{l'}$ for all valid index combinations and concludes the proof. ■

4 | THE LDD-TPR SOLVER FOR THE MULTIDOMAIN CASE

In this section we provide a generalization of Problem 2 to a multidomain setting. An in-depth presentation with a multidomain convergence result can be found in [36, Section 4.4].

We start with a generalization of our geometric notation. The domain $\Omega \subset \mathbb{R}^d$ is partitioned into a finite number of non-overlapping Lipschitz subdomains $\Omega_l \subset \Omega$ such that $\overline{\Omega} = \cup_{l=1}^W \overline{\Omega_l}$. The interior of intersections of the boundary of neighboring domains, $\Gamma_{kl} := \overline{\Omega_k} \cap \overline{\Omega_l} \backslash \partial\left(\overline{\Omega_k} \cup \overline{\Omega_l}\right)$ that in addition have non-zero $(d-1)$-dimensional Hausdorff measure are called interfaces and are submanifolds of dimension $d-1$. As a consequence, the outer normal $\boldsymbol{n_{kl}} \in S^{d-1}$ pointing from Ω_k to Ω_l is defined almost everywhere on Γ_{kl}, compare [34, p. 97 ff.] and [6] for more details on definitions. Figure 2b, p. 18, illustrates the notation. Given Ω_l, let $\mathcal{I}_l \subset \mathcal{I} = \{1, \ldots, W\}$ be the set of indices denoting those neighboring subdomains Ω_k for which Γ_{lk} is an interface. Furthermore, let $\Gamma_l := \operatorname{int}\left(\partial\Omega \cap \overline{\Omega_l}\right)$ denote that particular part of the boundary of Ω_l intersecting with $\partial\Omega$ for all $l \in \mathcal{I}$ for which Γ_l is $(d-1)$-dimensional. Then $\partial\Omega = \cup_{l\in\mathcal{I}}\overline{\Gamma_l}$ and $\partial\Omega_l = \cup_{k\in\mathcal{I}_l}\left(\overline{\Gamma_{kl}} \cup \overline{\Gamma_l}\right)$.

Let $\mathcal{I}^R, \mathcal{I}^{TP} \subset \mathcal{I}$ with $\mathcal{I} = \mathcal{I}^R \dot\cup \mathcal{I}^{TP}$ be the (possibly empty) sets of indices denoting the subdomains Ω_l on which the Richards equation $\left(l \in \mathcal{I}^R\right)$ or the full two-phase system $\left(l \in \mathcal{I}^{TP}\right)$ is imposed. If neither $\mathcal{I}^R \neq \emptyset$ nor $\mathcal{I}^{TP} \neq \emptyset$, denote by $\mathcal{I}_R^{TP} \subset \mathcal{I}^{TP}$ the indices of domain patches, that model the full two-phase flow but have at least one neighboring subdomain that assumes the Richards model sharing an interface of dimension $(d-1)$. Similarly, define the subset $\mathcal{I}_{TP}^R \subset \mathcal{I}^R$ of Richards subdomains with a two-phase neighbor. Given a subdomain Ω_k with $k \in \mathcal{I}_R^{TP}$, let $\mathcal{I}_{k,R}^{TP} \subset \mathcal{I}_k$ be the set of indices of neighboring Richards subdomains. Analogously, for Ω_k with $k \in \mathcal{I}_{TP}^R$, let $\mathcal{I}_{k,TP}^R \subset \mathcal{I}_k$ be the set of indices of neighboring two-phase subdomains.

Turning to function spaces, we decompose $H_0^1(\Omega)$ into spaces

$$\mathcal{V}_l := \left\{u \in H^1(\Omega_l) \mid u|_{\partial\Omega_l\cap\partial\Omega} = 0\right\}$$

and set

$$\widehat{\mathcal{V}}^w := \prod_{j=1}^W \mathcal{V}_j, \quad \text{and} \quad \mathcal{V}^w = \left\{(u_1, \ldots, u_W) \in \widehat{\mathcal{V}}^w \mid u_l\big|_{\Gamma_{lk}} = u_k\big|_{\Gamma_{lk}}, l \in \mathcal{I}, k \in \mathcal{I}_l\right\},$$

the latter being $H_0^1(\Omega)$. In case Ω_k is an internal subdomain, that is, $\partial\Omega_k \cap \partial\Omega = \emptyset$, we have $\mathcal{V}_k = H^1(\Omega_k)$.

If a purely Richards or purely two-phase domain decomposition is considered, that is, no TP–R coupling occurs, the space $\mathcal{V}^w$ can be used for the wetting phases, (Richards) and also the nonwetting phases (two-phase). If both models are present, however, we refine the notion of $\mathcal{V}^{nw}$, the space for the nonwetting phase. For all $k \in \mathcal{I}^{TP}$ define $\mathcal{V}_l^{nw} := \mathcal{V}_l$, $\mathcal{V}_k^{nw} = \{0\}$ for $k \in \mathcal{I}^R$ and set the general space for the nonwetting phase

$$\widehat{\mathcal{V}}^{nw} := \prod_{j=1}^{W} \mathcal{V}_j \quad \text{and} \qquad \mathcal{V}^{nw} := \left\{ (u_1, \dots, u_W) \in \widehat{\mathcal{V}}^{nw} \,\middle|\, u_l\,|_{\Gamma_{lk}} = u_k|_{\Gamma_{lk}}, l \in \mathcal{I}^{TP} \right\}.$$

Note, that since for $k \in \mathcal{I}^R$ we set $\mathcal{V}_k^{nw} = \{0\}$, $u_l\,|_{\Gamma_{lk}} = u_k|_{\Gamma_{lk}}$ for $k \in \mathcal{I}_{l,R}^{TP}$ actually means $u_l|_{\Gamma_{lk}} = 0$. Lastly, in order to define Neumann traces, we need those subspaces of the spaces $\mathcal{V}_k^{\alpha}$ and $\mathcal{V}^{\alpha}$ for which traces on each interface to neighbors can be extended by zero. We set

$$\mathcal{V}_{k,00}^{\alpha} := \left\{ u \in \mathcal{V}_k^{\alpha} \,|\, u|_{\Gamma_{kl}} \in H_{00}^{1/2}(\Gamma_{kl}), l \in \mathcal{I}_k \right\} \quad \text{and} \quad \widehat{\mathcal{V}}_{00}^{\alpha} := \prod_{j=1}^{W} \mathcal{V}_{j,00}^{\alpha},$$

for $\alpha \in \{w, nw\}$.

With the above notations a multidomain semidiscrete formulation of Problem 2 reads as.

Problem 4 (Semidiscrete TP–R problem, multidomain) Given functions $\left(p_w^{n-1}, p_{nw}^{n-1}\right) \in \mathcal{V}^w \times \mathcal{V}^{nw}$, find $(p_w^n, p_{nw}^n) \in \mathcal{V}^w \times \mathcal{V}^{nw}$, such that all fluxes fulfill $\boldsymbol{F_{\alpha,l}^n} \cdot \boldsymbol{n_{lk}} \in H_{00}^{1/2}(\Gamma_{lk})'$ for $l \in \mathcal{I}$, $k \in \mathcal{I}_l$, $\alpha \in \{w, nw\}$, and the equations

$$\left\langle \Phi_l S_l^n - \Phi_l S_l^{n-1}, \varphi_{w,l} \right\rangle - \tau \left\langle \boldsymbol{F_{w,l}^n}, \nabla\varphi_{w,l} \right\rangle + \tau \sum_{k \in \mathcal{I}_l} \left\langle \boldsymbol{F_{w,k}^n} \cdot \boldsymbol{n_{lk}}, \varphi_{w,l} \right\rangle_{\Gamma_{lk}} = \tau \left\langle f_{w,l}^n, \varphi_{w,l} \right\rangle$$

as well as

$$\left\langle \Phi_j S_j^n - \Phi_j S_j^{n-1}, \varphi_{w,j} \right\rangle - \tau \left\langle \boldsymbol{F_{w,j}^n}, \nabla\varphi_{w,j} \right\rangle + \tau \sum_{k \in \mathcal{I}_j} \left\langle \boldsymbol{F_{w,k}^n} \cdot \boldsymbol{n_{jk}}, \varphi_{w,j} \right\rangle_{\Gamma_{jk}} = \tau \left\langle f_{w,j}^n, \varphi_{w,j} \right\rangle,$$

$$-\left\langle \Phi_j S_j^n - \Phi_j S_j^{n-1}, \varphi_{nw,j} \right\rangle - \tau \left\langle \boldsymbol{F_{nw,j}^n}, \nabla\varphi_{nw,j} \right\rangle + \tau \sum_{k \in \mathcal{I}_j} \left\langle \boldsymbol{F_{nw,k}^n} \cdot \boldsymbol{n_{jk}}, \varphi_{nw,j} \right\rangle_{\Gamma_{jk}} = \tau \left\langle f_{nw,j}^n, \varphi_{nw,j} \right\rangle$$

are satisfied for $l \in \mathcal{I}^R$, $j \in \mathcal{I}^{TP}$ and for all $\left(\varphi_{\alpha,1}, \varphi_{\alpha,2}, \dots, \varphi_{\alpha,W}\right) \in \widehat{\mathcal{V}}_{[00]}^{\alpha}$.

As we have seen in the previous section, compare Lemma 1, introducing a Robin type formulation allows to drop the pressure continuity that is implicitly contained in the definition of our spaces $\mathcal{V}^w$ and $\mathcal{V}^{nw}$. Instead, the pressure continuity becomes part of the equations to solve and is thereby more accessible to implementation. Setting analogously to equations (24)–(25) for $\lambda_\alpha^{lk} = \lambda_\alpha^{kl} > 0$

$$g_{\alpha,lk} := -\lambda_\alpha^{lk} p_{\alpha,l}^n\Big|_{\Gamma_{lk}} + \boldsymbol{F_{\alpha,l}^n} \cdot \boldsymbol{n_{lk}}, \quad (l \in \mathcal{I}), (k \in \mathcal{I}_l) \quad \text{and} \quad \alpha \in \{n, nw\},$$

in $H_{00}^{1/2}(\Gamma_{lk})'$, where as in the previous sections $g_{nw,lk} = \boldsymbol{F_{nw,l}^n} \cdot \boldsymbol{n_{lk}}$ on Richards subdomains $l \in \mathcal{I}^R$ are only nonzero if the neighbor Ω_k assumes the two-phase model, that is, $k \in \mathcal{I}_{l,TP}^R$ and gravity is included, Problem 4 can be equivalently reformulated into.

Problem 5 (Semidiscrete TP–R problem, limit formulation, multidomain) Let functions $\left(p_w^{n-1}, p_{nw}^{n-1}\right) \in \mathcal{V}^w \times \mathcal{V}^{nw}$ as well as real numbers $\lambda_\alpha^{lk} = \lambda_\alpha^{kl} > 0$ be given for all interfaces Γ_{lk}, $l \in \mathcal{I}$, $k \in \mathcal{I}_l$, and appearing phases α.

Find $(p_w^n, p_{nw}^n) \in \widehat{\mathcal{V}}^w \times \widehat{\mathcal{V}}^{nw}$ and $g_{\alpha,lk} \in H_{00}^{1/2}(\Gamma_{lk})'$, $l \in \mathcal{I}$, $k \in \mathcal{I}_l$, $\alpha \in \{w, nw\}$ such that on Richards domains, that is, $l \in \mathcal{I}^R$, the terms $g_{\alpha,lk}$ are given by

$$\begin{aligned} g_{nw,lk} &= \boldsymbol{F_{nw,l}^n} \cdot \boldsymbol{n_{lk}}, && \textit{for} \quad l \in \mathcal{I}_{TP}^R, \quad \textit{and} \quad k \in \mathcal{I}_{l,TP}^R, \\ g_{nw,lk} &= 0, && \textit{for} \quad l \in \mathcal{I}_{TP}^R \quad \textit{and} \quad k \in \mathcal{I}_l \backslash \mathcal{I}_{l,TP}^R, \\ g_{nw,lk} &= 0, && \textit{for} \quad l \in \mathcal{I}^R \backslash \mathcal{I}_{TP}^R, \quad \textit{and} \quad k \in \mathcal{I}_j, \end{aligned} \tag{62}$$

where $\boldsymbol{F^n_{nw,l}} \cdot \boldsymbol{n_{lk}} \in H^{1/2}_{00}(\Gamma_{lk})'$ are defined by the right hand side of either (6) or (7), and these functions (p^n_w, p^n_{nw}) and $g_{\alpha,lk}$ fulfill the equations

$$\left\langle \Phi_l S^n_l - \Phi_l S^{n-1}_l, \varphi_{w,l} \right\rangle - \tau \left\langle \boldsymbol{F^n_{w,l}}, \nabla \varphi_{w,l} \right\rangle + \sum_{k \in \mathcal{I}_l} \tau \left\langle \lambda^{lk}_w p^n_{w,l} + g_{w,lk}, \varphi_{w,l} \right\rangle_{\Gamma_{lk}} = \tau \left\langle f^n_{w,l}, \varphi_{w,l} \right\rangle, \tag{63}$$

for $l \in \mathcal{I}^R$ with

$$\langle g_{w,lk}, \varphi_{w,l} \rangle_{\Gamma_{lk}} = \left\langle -2\lambda^{lk}_w p^n_{w,k} - g_{w,kl}, \varphi_{w,l} \right\rangle_{\Gamma_{lk}} \quad (k \in \mathcal{I}_l), \tag{64}$$

$$\langle g_{nw,lk}, \varphi_{nw,k} \rangle_{\Gamma_{lk}} = \left\langle -2\lambda^{lk}_{nw} p^n_{nw,k} - g_{nw,kl}, \varphi_{nw,k} \right\rangle_{\Gamma_{lk}} \quad \left(k \in \mathcal{I}^R_{l,TP}\right), \tag{65}$$

and for $j \in \mathcal{I}^{TP}$ the equations

$$\left\langle \Phi_j S^n_j - \Phi_j S^{n-1}_j, \varphi_{w,j} \right\rangle - \tau \left\langle \boldsymbol{F^n_{w,j}}, \nabla \varphi_{w,j} \right\rangle + \tau \sum_{k \in \mathcal{I}_j} \left\langle \lambda^{jk}_w p^n_{w,l} + g_{w,jk}, \varphi_{w,j} \right\rangle_{\Gamma_{jk}} = \tau \left\langle f^n_{w,j}, \varphi_{w,j} \right\rangle, \tag{66}$$

$$-\left\langle \Phi_j S^n_j - \Phi_j S^{n-1}_j, \varphi_{nw,j} \right\rangle - \tau \left\langle \boldsymbol{F^n_{nw,j}}, \nabla \varphi_{nw,j} \right\rangle + \tau \sum_{k \in \mathcal{I}_j} \left\langle \lambda^{jk}_{nw} p^n_{nw,l} + g_{nw,jk}, \varphi_{nw,j} \right\rangle_{\Gamma_{jk}} = \tau \left\langle f^n_{nw,j}, \varphi_{nw,j} \right\rangle, \tag{67}$$

together with

$$\left\langle g_{w,jk}, \varphi_{w,j} \right\rangle_{\Gamma_{jk}} = \left\langle -2\lambda^{jk}_w p^n_{w,k} - g_{w,kj}, \varphi_{w,j} \right\rangle_{\Gamma_{jk}} \quad \left(k \in \mathcal{I}_j\right), \tag{68}$$

$$\left\langle g_{nw,jk}, \varphi_{w,j} \right\rangle_{\Gamma_{jk}} = \left\langle -2\lambda^{jk}_{nw} p^n_{nw,k} - g_{nw,kj}, \varphi_{nw,j} \right\rangle_{\Gamma_{jk}} \quad \left(k \in \mathcal{I}_j \cap \mathcal{I}^{TP}\right), \tag{69}$$

$$\left\langle g_{nw,jk}, \varphi_{nw,j} \right\rangle_{\Gamma_{jk}} = \left\langle -g_{nw,kj}, \varphi_{nw,j} \right\rangle_{\Gamma_{jk}} \quad \left(k \in \mathcal{I}^{TP}_{j,R}\right), \tag{70}$$

for all $\left(\varphi_{\alpha,1}, \varphi_{\alpha,2}, \dots, \varphi_{\alpha,W}\right) \in \widehat{\mathcal{V}}^{\alpha}_{[00]}$.

Remark 8 (Necessity of $\widehat{\mathcal{V}}^{\alpha}_{00}$ as test function space) In order to define Neumann traces on parts of a boundary $\Gamma \subset \partial\Omega$ of a Lipschitz domain Ω, test functions $\varphi \in H^{1/2}(\Gamma)$ need to be extendable by zero and these are precisely the functions in $H^{1/2}_{00}(\Gamma)$. If we tested the above problems with functions $\varphi_{\alpha,l} \in \mathcal{V}^{\alpha}_l$ the traces $\varphi_l|_{\Gamma_{lk}}$ for $k \in \mathcal{I}_l$ a priori would only lie in $H^{1/2}(\Gamma_{lk})$. For the Neumann traces appearing in Problems 4 and 5 to be well-defined, we need $\varphi_l|_{\Gamma_{lk}} \in H^{1/2}_{00}(\Gamma_{lk})$ for $k \in \mathcal{I}_l$, however. Testing with $\varphi_{\alpha,l} \in \widehat{\mathcal{V}}^{\alpha}_{00}$ precisely alleviates that problem.

As before, Problem 5 shows how to design the multidomain LDD-TP–R solver step.

Problem 6 (LDD-TP–R solver step, multidomain, version 1) Given $\left(p^{n-1}_w, p^{n-1}_{nw}\right) \in \mathcal{V}^w \times \mathcal{V}^{nw}$, set on all subdomains Ω_l, $l \in \mathcal{I}$, for some $L_{\alpha,l} > 0$ as initial iterates

$$p^{n,0}_{\alpha,l} := p^{n-1}_{\alpha,l}, \tag{71}$$

where $\alpha \in \{w\}$ for $l \in \mathcal{I}^R$ and $\alpha \in \{w, nw\}$ for $l \in \mathcal{I}^{TP}$ as well as

$$g^0_{\alpha,lk} := \boldsymbol{F^{n-1}_{\alpha,l}} \cdot \boldsymbol{n_{lk}} - \lambda^{lk}_{\alpha} p^{n-1}_{\alpha,l}\Big|_{\Gamma_{lk}} \tag{72}$$

in $H_{00}^{1/2}(\Gamma_{lk})'$ for $k \in \mathcal{I}_l$ and $\lambda_\alpha^{lk} = \lambda_\alpha^{kl} > 0$. As before, for Richards domains, Ω_l with $l \in \mathcal{I}^R$, and on interfaces Γ_{lk} to a two-phase domain, that is, $k \in \mathcal{I}_{l,TP}^R$, equation (72) becomes

$$g_{\alpha,lk}^0 := \boldsymbol{F}_{\boldsymbol{\alpha,l}}^{\boldsymbol{n\text{-}1}} \cdot \boldsymbol{n_{lk}} \tag{73}$$

and the fluxes $\boldsymbol{F}_{\boldsymbol{\alpha,l}}^{\boldsymbol{n\text{-}1}} \cdot \boldsymbol{n_{lk}}$ are defined by the right hand side of either (6) or (7). On interfaces Γ_{lk} between Richards domains, we take

$$g_{nw,lk}^0 = 0. \tag{74}$$

Given the iterates $\left(p_w^{n,i-1}, p_{nw}^{n,i-1}\right) \in \widehat{\mathcal{V}}^w \times \widehat{\mathcal{V}}^{nw}$, as well as $g_{\alpha,lk}^{i-1} \in H_{00}^{1/2}(\Gamma_{lk})'$, $(\mathbb{N} \in i \geq 1)$, one step of the LDD-TP–R solver consists of finding $\left(p_w^{n,i}, p_{nw}^{n,i}\right) \in \widehat{\mathcal{V}}^n \times \widehat{\mathcal{V}}_{nw}$ such that on Richards subdomains, that is, $l \in \mathcal{I}^R$, the equations

$$\begin{aligned} & L_{w,l}\left\langle p_{w,l}^{n,i}, \varphi_{w,l}\right\rangle - \tau\left\langle \boldsymbol{F}_{\boldsymbol{w,l}}^{\boldsymbol{n,i}}, \nabla\varphi_{w,l}\right\rangle + \tau\sum_{k\in\mathcal{I}_l}\left\langle \lambda_w^{lk} p_{w,l}^{n,i} + g_{w,lk}^i, \varphi_{w,l}\right\rangle_{\Gamma_{lk}} \\ & = L_{w,l}\left\langle p_{w,l}^{n,i-1}, \varphi_{w,l}\right\rangle - \left\langle \Phi_l S_l^{n,i-1} - \Phi_l S_l^{n-1}, \varphi_{w,l}\right\rangle + \tau\left\langle f_{w,l}^n, \varphi_{w,l}\right\rangle, \end{aligned} \tag{75}$$

with

$$\left\langle g_{w,lk}^i, \varphi_{w,l}\right\rangle_{\Gamma_{lk}} := \left\langle -2\lambda_w^{lk} p_{w,k}^{n,i-1} - g_{w,kl}^{i-1}, \varphi_{w,l}\right\rangle_{\Gamma_{lk}} \quad (k \in \mathcal{I}_l), \tag{76}$$

$$\left\langle g_{nw,lk}^i, \varphi_{nw,k}\right\rangle_{\Gamma_{lk}} := \left\langle -2\lambda_{nw}^{lk} p_{nw,k}^{n,i-1} - g_{nw,kl}^{i-1}, \varphi_{nw,k}\right\rangle_{\Gamma_{lk}} \quad \left(k \in \mathcal{I}_{l,TP}^R\right) \tag{77}$$

are satisfied, and on two-phase domains, $\left(j \in \mathcal{I}^{TP}\right)$, the equations

$$\begin{aligned} & L_{\alpha,j}\left\langle p_{\alpha,j}^{n,i}, \varphi_{\alpha,j}\right\rangle - \tau\left\langle \boldsymbol{F}_{\boldsymbol{\alpha,j}}^{\boldsymbol{n,i}}, \nabla\varphi_{\alpha,j}\right\rangle + \tau\sum_{k\in\mathcal{I}_j}\left\langle \lambda_\alpha^{jk} p_{\alpha,j}^{n,i} + g_{\alpha,jk}^i, \varphi_{\alpha,j}\right\rangle_{\Gamma_{jk}} \\ & = L_{\alpha,j}\left\langle p_{\alpha,j}^{n,i-1}, \varphi_{\alpha,j}\right\rangle + (-1)^{\delta_{\alpha w}}\left\langle \Phi_j S_j^{n,i-1} - \Phi_j S_j^{n-1}, \varphi_{\alpha,j}\right\rangle + \tau\left\langle f_{\alpha,2}^n, \varphi_{\alpha,j}\right\rangle, \end{aligned} \tag{78}$$

for $\alpha \in \{n, nw\}$ along with

$$\left\langle g_{w,jk}^i, \varphi_{w,j}\right\rangle_{\Gamma_{jk}} := \left\langle -2\lambda_w^{jk} p_{w,k}^{n,i-1} - g_{w,kj}^{i-1}, \varphi_{w,j}\right\rangle_{\Gamma_{jk}} \quad \left(k \in \mathcal{I}_j\right), \tag{79}$$

$$\left\langle g_{nw,jk}^i, \varphi_{w,j}\right\rangle_{\Gamma_{jk}} := \left\langle -2\lambda_{nw}^{jk} p_{nw,k}^{n,i-1} - g_{nw,kj}^{i-1}, \varphi_{nw,j}\right\rangle_{\Gamma_{jk}} \quad \left(k \in \mathcal{I}_j \cap \mathcal{I}^{TP}\right), \tag{80}$$

$$\left\langle g_{nw,jk}^i, \varphi_{nw,j}\right\rangle_{\Gamma_{jk}} := \left\langle -g_{nw,kj}^{i-1}, \varphi_{nw,j}\right\rangle_{\Gamma_{jk}} \quad \left(k \in \mathcal{I}_{j,R}^{TP}\right) \tag{81}$$

are fulfilled for all test functions $(\varphi_w, \varphi_{nw}) \in \widehat{\mathcal{V}}_{00}^w \times \widehat{\mathcal{V}}_{00}^{nw}$.

Remark 9 We note that the iterates $\left(p_w^{n,i}, p_{nw}^{n,i}\right)$ are only required to be in $\widehat{\mathcal{V}}^w \times \widehat{\mathcal{V}}^{nw}$ and need not to be in $\mathcal{V}^w \times \mathcal{V}^{nw}$ (the latter meaning continuity over interfaces). If the family of subsequent solutions to the LDD-TP–R solver step, Problem 8, converge to a solution of Problem 5, then the continuity of the pressures is guaranteed in the limit.

From the proof of Theorem 1 we expect that the convergence of the solver holds also in the multidomain case irrespectively of the choice of initial iterates. Therefore, it is possible to choose other initial iterates than given in (71) and (72). In particular, $g_{\alpha,lk}^0$ can instead be chosen to belong to $H^{1/2}(\Gamma_{lk})'$

providing $g^i_{\alpha,lk} \in H^{1/2}(\Gamma_{lk})'$ as well, and Problem 6 can be tested with functions $(\varphi_w, \varphi_{nw}) \in \hat{\mathcal{V}}^w \times \hat{\mathcal{V}}^{nw}$ instead of $(\varphi_w, \varphi_{nw}) \in \hat{\mathcal{V}}^w_{00} \times \hat{\mathcal{V}}^{nw}_{00}$. While in general it is not clear whether it is possible to approximate the Neumann fluxes in Problem 5 by functionals in $H^{1/2}_{00}(\Gamma_{lk})'$, in situations, where $\hat{\mathcal{V}}^w \times \hat{\mathcal{V}}^{nw}$ can be chosen as test function space, it is useful to do so for two reasons. First, this makes the Lax–Milgram arguments from Lemma 3 carry over to the multidomain situation here, so that a solution to each iteration of the solver can be guaranteed. Secondly, implementation is facilitated, as the requirement $(\varphi_w, \varphi_{nw}) \in \hat{\mathcal{V}}^w_{00} \times \hat{\mathcal{V}}^{nw}_{00}$ is more difficult to achieve in an implementation than $(\varphi_w, \varphi_{nw}) \in \hat{\mathcal{V}}^w \times \hat{\mathcal{V}}^{nw}$. Thus, a more practical formulation of the LDD-TP–R solver used in Section 5 below is given by.

Problem 8 (LDD-TP–R solver step, multidomain, version 2) Let functions $\left(p^{n-1}_w, p^{n-1}_{nw}\right) \in \mathcal{V}^w \times \mathcal{V}^{nw}$ be given and define on all subdomains Ω_l, $l \in \mathcal{I}$, for arbitrary $v^\alpha_l \in \mathcal{V}^\alpha_l$ and $\zeta^\alpha_{lk} \in H^{1/2}_{00}(\Gamma_{lk})'$, $k \in \mathcal{I}_l$, as initial iterates

$$p^{n,0}_{\alpha,l} := v^\alpha_l,$$

where $\alpha \in \{w\}$ for $l \in \mathcal{I}^R$ and $\alpha \in \{w, nw\}$ for $l \in \mathcal{I}^{TP}$ as well as

$$g^0_{\alpha,lk} := \zeta^\alpha_{lk}$$

in $H^{1/2}_{00}(\Gamma_{lk})'$. On interfaces Γ_{lk} between Richards domains, we take

$$g^0_{nw,lk} = 0.$$

In addition, choose on each domain Ω_l, $l \in \mathcal{I}$, some real number $L_{\alpha,l} > 0$ and on all interfaces Γ_{lk}, $k \in \mathcal{I}_l$, real numbers $\lambda^{lk}_\alpha = \lambda^{kl}_\alpha > 0$. Given previously known iterates $\left(p^{n,i-1}_w, p^{n,i-1}_{nw}\right) \in \hat{\mathcal{V}}^w \times \hat{\mathcal{V}}^{nw}$, as well as $g^{i-1}_{\alpha,lk} \in H^{1/2}_{00}(\Gamma_{lk})'$, $(\mathbb{N} \in i \geq 1)$, one step of the LDD-TP–R solver consists of finding $\left(p^{n,i}_w, p^{n,i}_{nw}\right) \in \hat{\mathcal{V}}^w \times \hat{\mathcal{V}}^{nw}$ such that on Richards subdomains, $l \in \mathcal{I}^R$, the equations (75) together with (76), (77) are satisfied, and on two-phase domains, $j \in \mathcal{I}^{TP}$, the equations (78) for $\alpha \in \{n, nw\}$ along with (79), (80), and (81) are fulfilled for all test functions $(\varphi_w, \varphi_{nw}) \in \hat{\mathcal{V}}^w \times \hat{\mathcal{V}}^{nw}$.

Remark 10 Note that the key difference between Problems 6 and 8 is the test function space and consequently the space on which the functionals $g^i_{\alpha,l}$ act.

5 | NUMERICAL VALIDATION OF THE LDD-TP–R SOLVER

In this section, we turn to the numerical validation of the LDD-TP–R solver for the case $d = 2$. We provide examples for two different substructurings. For a two-domain case, we compare the performance of the LDD-TP–R solver to the full two-phase flow model. In addition, we discuss the choice of solver parameters. For a multidomain example involving an inner subdomain, we illustrate the performance as well. Both domain partitions are displayed in Figure 2.

All experiments were implemented using Python and Fenics' main library Dolfin, compare [38, 39]. The code for all examples along with its documentation can be found at [40].

For a detailed description of the design principles we refer to [36]. Here we restrict ourselves to a listed summary regarding the grid and the ansatz functions.

SUBSTRUCTURING AND MESHES. All subdomains $\Omega_l \subset \Omega \subset \mathbb{R}^2$ and triangular meshes are constructed by the Fenics mesh tool Mshr. To ensure that the meshes are matching, submeshes $\mathcal{T}_l$ on each subdomain Ω_l are always extracted from a global conforming mesh $\mathcal{T}$ on Ω. This means, mesh

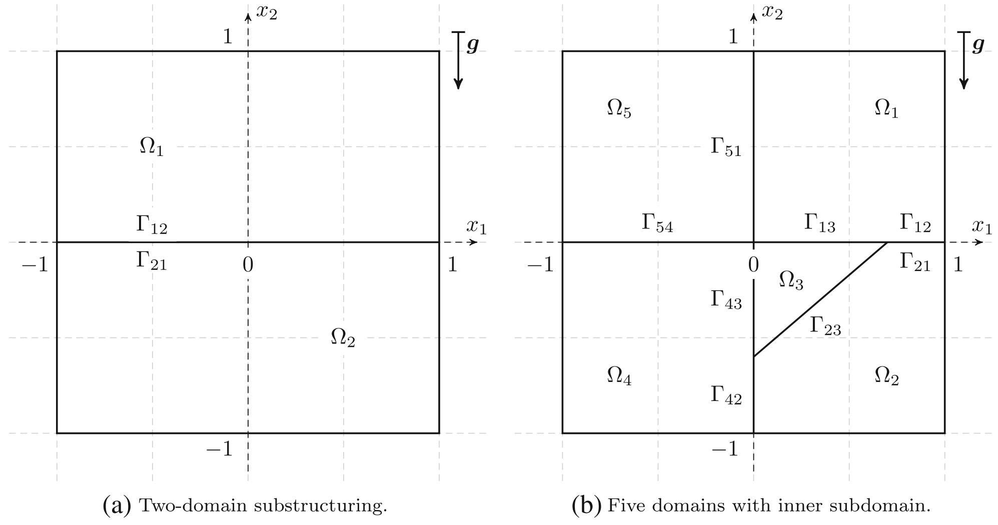

FIGURE 2 Domains used in the numerical experiments. All domains are polygonal subdivisions of the unit square $[0, 1] \times [0, 1]$. The nomenclature of the interfaces follows the conventions introduced in Section 4

vertices and faces always lie on the polygons defining the interfaces, and no facets intersect interfaces. In this way, neighboring subdomains share vertices and facets over interfaces. Dolfin was instructed to use ParMETIS as mesh partitioner. An example of such a mesh can be seen in Figure 7b). If d_Δ is the diameter (two times the circumradius) of a mesh cell (triangle) $\Delta \in \mathcal{T}_l$, the mesh size h_l on each domain is defined as $h_l = \max\{d_\Delta \mid \Delta \in \mathcal{T}_l\}$.

On each subdomain mesh, Fenics' first-order Lagrange finite elements, $\mathcal{P}_1\Lambda^0$, were used as ansatz spaces $\mathcal{V}_{h,l} \subset \mathcal{V}_l$.

INTERFACES TERMS AND COMMUNICATION. The calculation of the Robin-interface terms across interfaces and the data exchange across interfaces requires manual assembly of the fluxes involving gradients of $\mathcal{P}_1\Lambda^0$ functions. The calculation of interface terms is done dof-wise and their communication over interfaces needs to take into account the different mesh and dof numberings on each subdomain adjacent to a given interface. The calculation of the approximations $g^{h,i}_{\alpha,lk}$ of the $g^{i}_{\alpha,lk}$-terms uses discontinuous Galerkin elements of degree 1, $\mathcal{P}_1\Lambda^2$. The reason is twofold. On the one hand, the calculation of $g^{h,0}_{\alpha,lk}$ necessitates the assembly of fluxes (since we use the initial iterates of Problem 6), involving thereby the gradient of a P_1 function, hence the need for discontinuous ansatz functions, and on the other hand it seemed desirable to have the same number of degrees of freedom as the pressures that need to be added to these terms.

The implementation of the $g^{h,i}_{\alpha,lk}$ terms is done in the following way. The LDD solver, upon entering time step n, first assembles $g^{h,0}_{\alpha,lk}$: On each domain Ω_l, $l \in \mathcal{I}$, the approximation $\boldsymbol{F}^{h,n-1}_{\alpha,l}$ of the flux $\boldsymbol{F}^{n-1}_{n,l}$ is assembled in $\mathcal{P}_1\Lambda^2 \times \mathcal{P}_1\Lambda^2$ and $\boldsymbol{F}^{h,n-1}_{\alpha,l} \cdot \boldsymbol{n}_{lk} \in \mathcal{P}_1\Lambda^2$ is added dof-wise to $p^{h,n-1}_{\alpha,l}\Big|_{\Gamma_{lk}}$ for dofs that lie on facets belonging to the interface Γ_{lk}, $k \in \mathcal{I}_l$. The resulting dofs of the $g^{h,0}_{\alpha,l}$-term are then saved to interface dictionaries for communication. During the ith iteration of the LDD solver on Ω_l, the $g^{h,i-1}_{\alpha,kl}$ and $p^{h,i-1}_{\alpha,k}$ dofs of the neighbor k are read from these interface dictionaries and are added—again dof-wise—along Γ_{lk} to get $g^{h,i}_{\alpha,lk} \in \mathcal{P}_1\Lambda^2$. Since the form assembly of Problem 8 is done in $\mathcal{P}_1\Lambda^0$, the $g^{h,i}_{\alpha,lk}$ terms enter the form as projections $\Pi g^{h,i}_{\alpha,lk} \in \mathcal{P}_1\Lambda^0$, where $\Pi : \mathcal{P}_1\Lambda^2 \to \mathcal{P}_1\Lambda^0$ is the projection onto $\mathcal{P}_1\Lambda^0$.

TABLE 1 TP–R coupling on two domains: coefficient functions and exact solutions

Data	Ω_1	Ω_2
$k_{w,l}(s)$	s^2	s^3
$k_{nw,l}(s)$	$(1-s)^2$	$(1-s)^3$
$S_l\,(p_c)$	$\begin{cases} \frac{1}{(1+p_c)^{\frac{1}{2}}} & p_c \geq 0 \\ 1 & p_c < 0 \end{cases}$	$\begin{cases} \frac{1}{(1+p_c)^{1/3}} & p_c \geq 0 \\ 1 & p_c < 0 \end{cases}$
$p^e_{w,l}(x,y,t)$	$-7-\left(1+t^2\right)\left(1+x^2+y^2\right)$	$-7-\left(1+t^2\right)\left(1+x^2\right)$
$p^e_{nw,l}(x,y,t)$	-	$\left(-2-t\left(1.1+y+x^2\right)\right)y^2$

All appearing linear systems were solved using the Generalized Minimal Residual Method (GMRES) in conjunction with Incomplete LU preconditioning (ILU) as realized in the Fenics library. We will use the following.

Notation 1 By $p^e_{\alpha,l}$ we denote manufactured solutions, and $p^{e,n}_{\alpha,l} := p^e_{\alpha,l}(\cdot,\cdot,t_n)$ are their evaluation at time step t_n. We have $p^{e,n}_{\alpha,l} = p^n_{\alpha,l}$ since manufactured solutions solve the semidiscrete TP–R problem. Numerical approximations are denoted with an additional h, that is, $p^{h,n}_{\alpha,l}$ is the numerical approximation of $p^{e,n}_{\alpha,l}/p^n_{\alpha,l}$ and the symbols $p^{h,i}_{\alpha,l}$ denote the numerical approximation of the iterates $p^{n,i}_{\alpha,l}$ of the LDD-TP–R solver. Note, that the index n is dropped in this case. This means that $p^{h,i}_{\alpha,l}$ always denotes the iterates in the calculation of the nth time step.

5.1 | Two-domain computations

Remark 11 (Choice of λ_α) So far we have not addressed how to choose the parameters λ_α appearing in the LDD-TP–R scheme since no restrictions on these parameters were necessary for the convergence analysis. Analysis on how to choose these parameters for optimal convergence rates exists for linear elliptic and parabolic problems as well as for the Stokes problem, see [22], [23], [24], and [25] as well as references therein. However, it is not clear in our nonlinear case whether an optimal choice exists and how to choose it. For the Richards-Richards case an optimal choice was found through numerical experimentation, see [1], but for the present case this is an open question. We therefore chose parameters through experimentation throughout this section.

We start the numerical validation of the LDD-TP–R solver for the two-domain case shown in Figure 2a.

5.1.1 | Homogeneous intrinsic permeability and porosity

We assume the permeability and porosity in both domains to be the same and demonstrate the convergence of the scheme using a manufactured solution. Modeling the flow of water and air, all soil parameters are listed in Table 2a. For the relative permeabilities, S-p_c relationships as well as the manufactured solution expressions we refer to Table 1.

Figure 3 shows the results for a simulation over 1500 time steps of size $\tau = 0.001$ on the time interval $[0,T] = [0,1.5]$ using a mesh size $h \approx 0.071$. The algorithm was set to terminate after the

TABLE 2 TP–R coupling on two domains: soil parameters for same (a) and varying (b) intrinsic permeabilities and porosities

(a) TP–R coupling on two domains: soil parameters for the case with same intrinsic permeabilities and porosities				
Parameter	Ω_1		Ω_2	
Φ_l	0.22		0.22	
$k_{i,l}$	0.01		0.01	
α	w	nw	w	nw
μ_α[kg/(ms)]	1	-	1	$\frac{1}{50}$
ρ_α $\left[\mathrm{kgm}^{-3}\right]$	997	-	997	1.225

(b) TP–R coupling on two domains: case with varying intrinsic permeabilities and porosities				
Parameter	Ω_1		Ω_2	
Φ_l	0.22		0.022	
$k_{i,l}$	0.01		0.0001	
α	w	nw	w	nw
μ_α[kg/(ms)]	1	$\frac{1}{50}$	1	$\frac{1}{50}$
ρ_α $\left[\mathrm{kgm}^{-3}\right]$	997	1.225	997	1.225

stopping criterion

$$\|p_{\alpha,l}^{h,i} - p_{\alpha,l}^{h,i-1}\|_2 < \varepsilon_s := 2 \cdot 10^{-6}$$

had been reached for all appearing l and α. Parameters of the TP–R solver were chosen as $L_{w,1} = 0.007$ and $L_{\alpha,2} = 0.005$ for all phases $\alpha \in \{w, nw\}$ and $\lambda_w^{12} = \lambda_{nw}^{12} = 0.75$. Figure 3a shows the relative error norms with respect to the exact solution over time, demonstrating that the accuracy remains invariant over time. The relative error of the nonwetting phase remains steadily around 0.009, that of the wetting phases below 0.01%. The nonwetting phase shows a greater approximation error, which is not unexpected, since no nonwetting phase equation is assumed in Ω_1. Figure 3b displays the errors of the solver for the time step 1500 at time $T = 1.5$.

To determine how the use of the TP–R coupling in this situation affects both accuracy and performance, we compare with a simulation of the same setting, assuming constant nonwetting pressure, $p_{nw,1} \equiv 0$ on Ω_1 and use the LDD solver for two-phase flow equations in Ω_1 and Ω_2 (LDD-TP–TP solver, see [2] for details). As Figure 3c shows, the same precision is achieved in both cases, using either the LDD-TP–R or the LDD-TP–TP solver. The worst relative error can be observed for the nonwetting phase on Ω_2, similarly to the case of the TP–R coupling shown in Figure 3a. This suggests that the error is not dominated by the use of the TP–R coupling in place of the a complete TP–TP coupling.

Naturally, the LDD-TP–TP solver is slower, having to solve an additional system. The subsequent errors at a fixed time step, Figure 3d, show in addition, that the LDD-TP–TP solver needs 199 iterations in the 1500th time step to achieve the same stopping criterion. 29 iterations were needed in the first time step.

These results show that in situations in which the assumptions for the validity of the Richards equation hold, the hybrid LDD-TP–R solver excels over the LDD-TP–TP solver as there is a noticeable performance gain at virtually no loss of approximation accuracy.

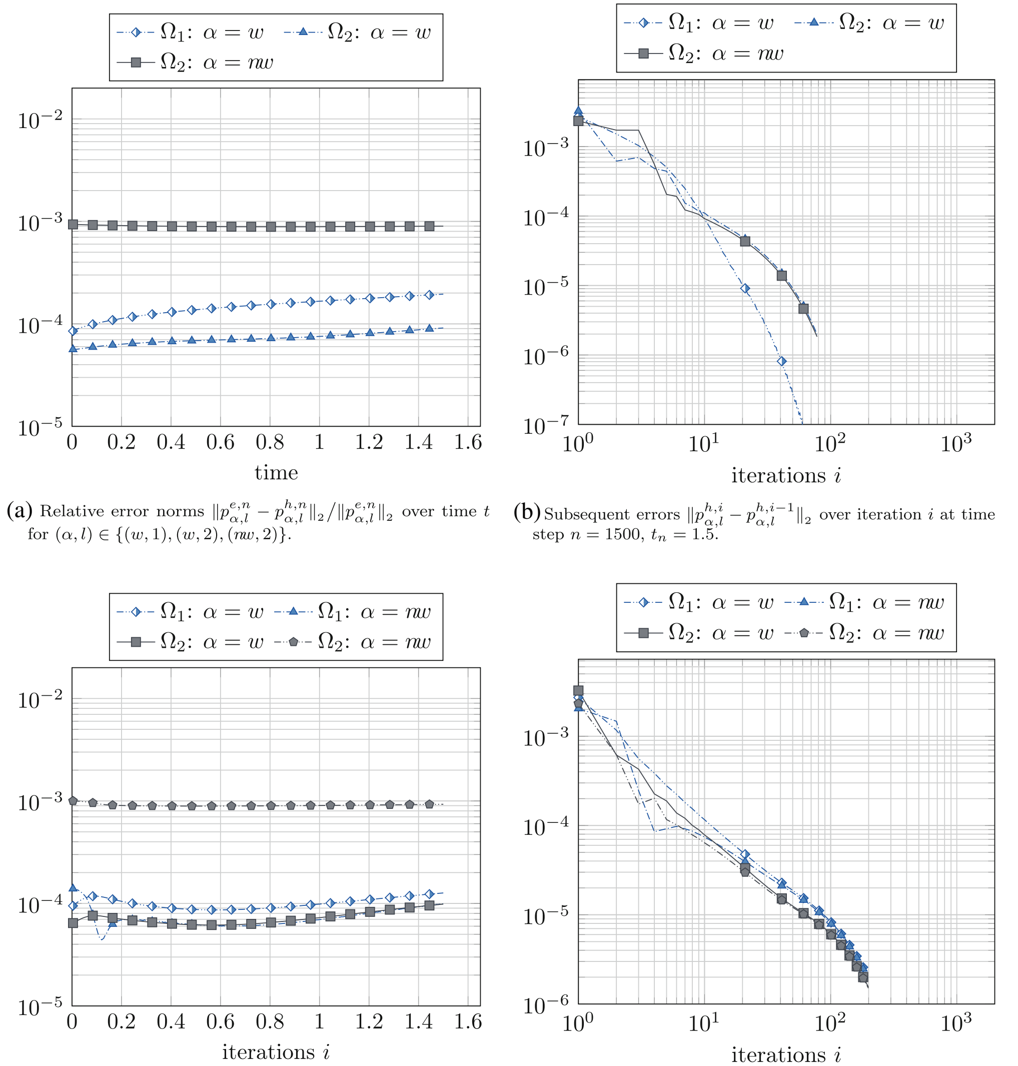

(a) Relative error norms $\|p^{e,n}_{\alpha,l} - p^{h,n}_{\alpha,l}\|_2 / \|p^{e,n}_{\alpha,l}\|_2$ over time t for $(\alpha, l) \in \{(w,1),(w,2),(nw,2)\}$.

(b) Subsequent errors $\|p^{h,i}_{\alpha,l} - p^{h,i-1}_{\alpha,l}\|_2$ over iteration i at time step $n = 1500$, $t_n = 1.5$.

(c) Relative error norms $\|p^{e,n}_{\alpha,l} - p^{h,n}_{\alpha,l}\|_2 / \|p^{e,n}_{\alpha,l}\|_2$ over time t for $\alpha \in \{w, nw\}$ and $l \in \{1,2\}$.

(d) Subsequent errors $\|p^{h,i}_{\alpha,l} - p^{h,i-1}_{\alpha,l}\|_2$ over iteration i at time step $n = 1500$, $t_n = 1.5$.

FIGURE 3 TP–R coupling on two domains: Relative error norms (a) and subsequent errors at a fixed time step (b) for a simulation over 1500 time steps with same intrinsic permeabilities and porosities, and parameters $h \approx 0.071$, $\tau = 1 \cdot 10^{-3}$, $L_{w,1} = 0.007$ and $L_{\alpha,2} = 0.005$, $\alpha \in \{w, nw\}$ and $\lambda^{12}_w = \lambda^{12}_{nw} = 0.75$. Relative error norms (c) and subsequent errors at a fixed time step (d) for a simulation of the same situation using the same parameters, but assuming a TP–TP coupling and assumed zero nonwetting phase

5.1.2 | Heterogeneous intrinsic permeabilities and porosities

We investigate numerically the influence of heterogeneous soil parameters running a test case with varying intrinsic permeabilities and porosities. The values used are listed in Table 2b. Relative permeabilities, p_c–S relationships and the exact solutions are the same as before, compare Table 1. Grid parameters remain the same, namely $h \approx 0.071$, and $\tau = 0.001$ for the time step. Figure 4 shows results for a simulation comprising 1500 time steps using LDD-TP–R parameters $\lambda^{12}_\alpha = 0.5$, $L_{w,1} = 0.007$, and $L_{\alpha,2} = 0.0005$, for $\alpha \in \{w, nw\}$. The stopping criterion was set to $\varepsilon_s = 2 \cdot 10^{-6}$. As can be seen from Figure 4a the final approximation precision is unaffected by the more challenging soil parameters

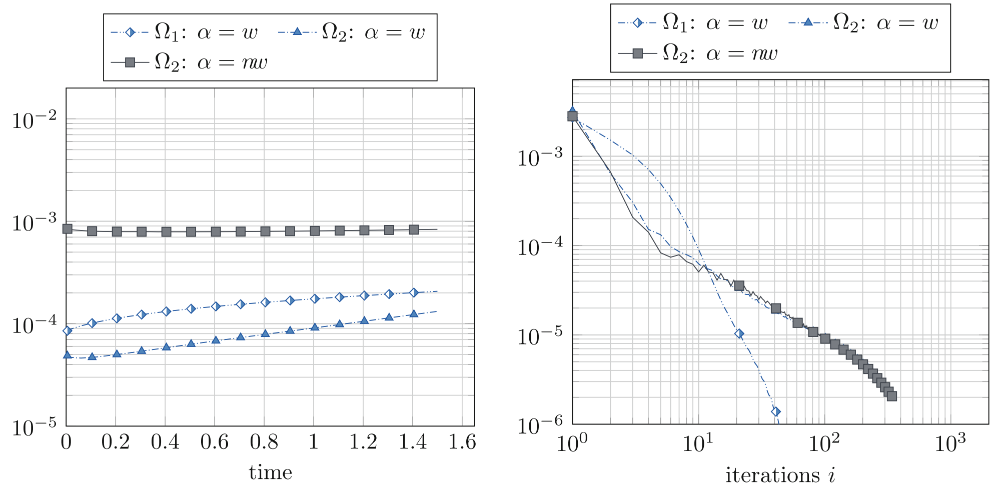

(a) Relative error norms $\|p^{e,n}_{\alpha,l} - p^{h,n}_{\alpha,l}\|_2 / \|p^{e,n}_{\alpha,l}\|_2$ over time t for $(\alpha, l) \in \{(w,1),(w,2),(nw,2)\}$.

(b) Subsequent errors $\|p^{h,i}_{\alpha,l} - p^{h,i-1}_{\alpha,l}\|_2$ over iteration i at time step $n = 1500$, $t_n = 1.5$.

FIGURE 4 TP–R coupling on two domains: Relative error norms (a) and subsequent errors at a fixed time step (b) for a simulation over 1500 time steps with varying intrinsic permeabilities and porosities, *excluding gravity* and parameters $h \approx 0.071$, $\tau = 1 \cdot 10^{-3}$, $\lambda^{12}_{\alpha} = 0.5$, $L_{w,1} = 0.007$ and $L_{\alpha,2} = 0.0005$, for $\alpha \in \{w, nw\}$

compared to the case with same intrinsic permeabilities. Mind the adjusted LDD-TP–R parameters $L_{\alpha,l}$ and λ^{12}_{α}, however, which needed to be adjusted to stabilize the iteration. This was a general trend observed in the experiments: The parameters need to be adapted to the situation specifically when heterogeneous parameters were used, see also [36] for more examples on this. In contrast to the previously shown case more iterations are needed to achieve the stopping criterion precision as is visible in Figure 4b. Required iterations ranged from 63 iterations in the first time step to 348 iterations in time step 1500 shown in Figure 4b.

5.1.3 | Comparison to coarser time step size

Figure 5a,b shows the same situation but simulated with a coarser time step $\tau = 1 \cdot 10^{-2}$ reaching $T = 15$ after 1500 iterations. Interestingly, the error norms of all phases are in the same range as for the simulation with the finer time step, compare Figure 5a, albeit the errors of the wetting phases behaving noticeably worse. The increase of error that starts taking place around $T = 10$ is due to solver maxing out the maximal iterations number, 1000. After $t = 10$ the solver always iterates 1000 times but fails to reach the stopping criterion. The effect is shown in Figure 5bc depicting the 1000 iterations in time step t_{1500} that the solver uses without reducing the subsequent errors sufficiently. Notably, convergence is very slow.

To compare the behavior of the solver at a similar time than is depicted in Figures 4b, 5b shows the behavior of the solver at $t = 1,67$. 141 iterations were used to achieve the error tolerance $\varepsilon_s = 1 \cdot 10^{-6}$. This means that up to this point in time, the LDD-TP–R solver needs less iterations in each time step of the simulation using $\tau = 0.01$ than in the example using $\tau = 0.001$, all the while achieving the same level of approximation error!

5.1.4 | Influence of LDD-TP–R parameters

The LDD solver is sensitive to the numerical parameters. To illustrate this dependence, we revisit the previous example with varying permeabilities and porosities keeping the grid parameters the same, but varying the LDD-TP–R parameters: Figure 6 shows results of a simulation of 800 time steps using

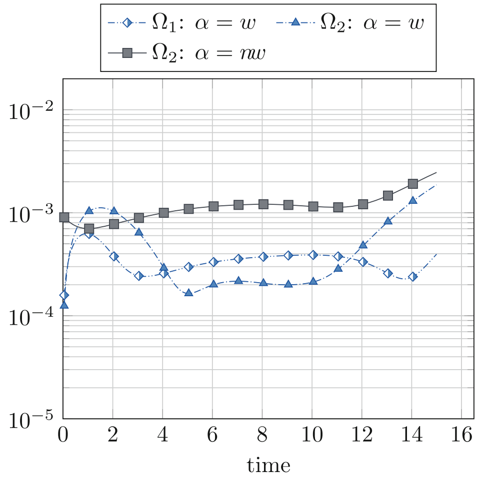

(a) Relative error norms $\|p^{e,n}_{\alpha,l} - p^{h,n}_{\alpha,l}\|_2 / \|p^{e,n}_{\alpha,l}\|_2$ over time t for $(\alpha, l) \in \{(w,1),(w,2),(nw,2)\}$.

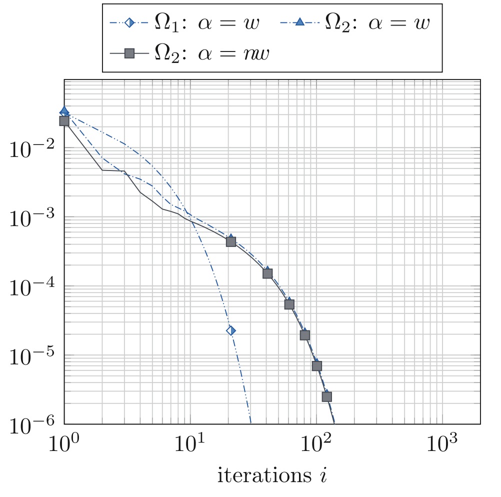

(b) Subsequent errors $\|p^{h,i}_{\alpha,l} - p^{h,i-1}_{\alpha,l}\|_2$ over iteration i at time step $n = 167$, $t_n = 1.67$.

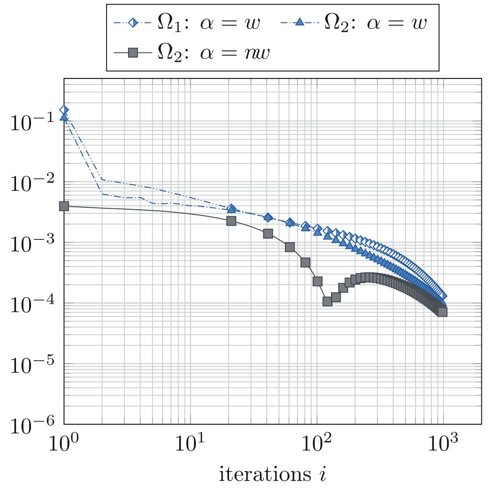

(c) Subsequent errors $\|p^{h,i}_{\alpha,l} - p^{h,i-1}_{\alpha,l}\|_2$ over iteration i at time step $n = 1500$, $t_n = 15$.

FIGURE 5 TP–R coupling on two domains: Relative error norms (a) and subsequent errors at a fixed time step (b) and (c) for the same situation as in Figure 4 simulated using a *coarser time step* $\tau = 1 \cdot 10^{-2}$

$\lambda^{12}_{\alpha} = 4$, $L_{w,1} = 0.025$ and $L_{w,2} = 0.05$, $L_{nw,2} = 0.025$ as well as $\varepsilon_s = 3 \cdot 10^{-6}$ as the stopping criterion. While the wetting phase error on Ω_1 at around 0.01% compares to the one in Figure 4a, Figure 6a shows that the errors of both phases on Ω_2 are an order of magnitude worse than what has been shown in Figure 4a. Accordingly, Figure 6b indicates by the high number of required iterations as well as the tilts observable in the subsequent error plots of the phases on Ω_2 that the solver struggles to find the solution. The required iterations to achieve the stopping criterion in this case ranged from 40 in the first time step to 577 in the 800th time step depicted in Figure 6b.

5.2 | Multidomain computations

We advance from the two-domain examples to a multidomain example featuring an inner subdomain, see Figure 2b. We assume the Richards equation on subdomains 1, 5 and the full two-phase flow model

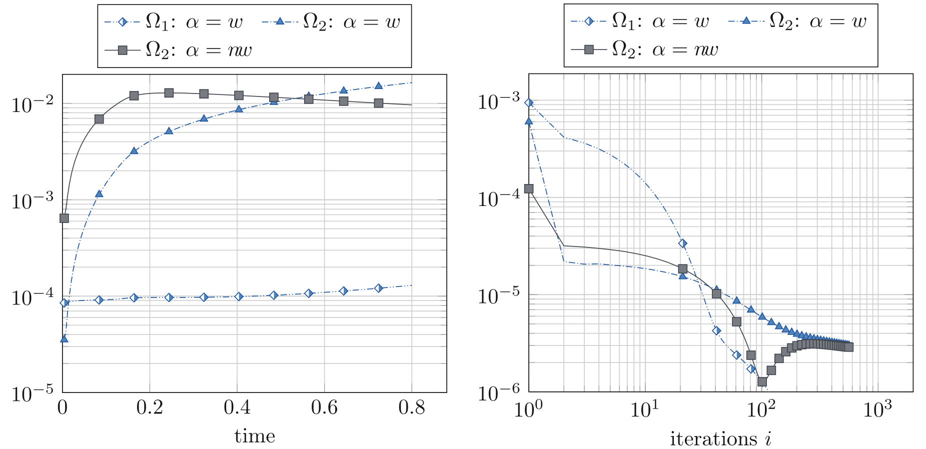

(a) Relative error norms $\|p^{e,n}_{\alpha,l} - p^{h,n}_{\alpha,l}\|_2 / \|p^{e,n}_{\alpha,l}\|_2$ over time t for $(\alpha, l) \in \{(w,1),(w,2),(nw,2)\}$. (b) Subsequent errors $\|p^{h,i}_{\alpha,l} - p^{h,i-1}_{\alpha,l}\|_2$ over iteration i at time step $n = 800$, $t_n = 0.8$.

FIGURE 6 TP–R coupling on two domains: Relative error norms (a) and subsequent errors at a fixed time step (b) for a simulation over 800 time steps with varying intrinsic permeabilities and porosities, and parameters $h \approx 0.071$, $\tau = 1 \cdot 10^{-3}$, $\lambda^{12}_{\alpha} = 4$, $L_{w,1} = 0.025$ and $L_{w,2} = 0.05$, $L_{nw,2} = 0.025$

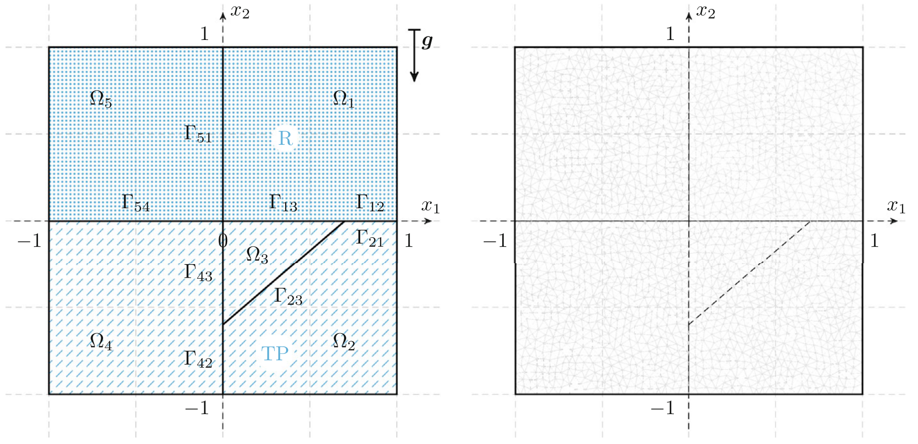

(a) Five domains with inner subdomain and highlighted model change. (b) Unstructured mesh for the five domain substructuring at `mesh_resolution` = 32.

FIGURE 7 TP–R coupling on a five domain substructuring. Highlighted are the areas where different models are being used (a). The dotted areas features Richards equations and the striped areas the two-phase flow model. Unstructured triangular mesh (b) for `mesh_resolution` = 32

on subdomains 2–4. The inner subdomain is Ω_3. According to Section 4, this means $\mathcal{I} = \{1, 2, 3, 4, 5\}$, $\mathcal{I}^R = \{1, 5\}$ and $\mathcal{I}^{TP} = \{2, 3, 4\}$, compare illustration in Figure 7a.

5.2.1 | Excluding gravity

We first use an example excluding gravity featuring the manufactured solutions, relative permeabilities and p_c–S-relations given in Table 3. Soil parameters are listed in Table 4. Notice that the same porosity $\Phi_l = 0.2$ and intrinsic permeability $k_{i,l} = 0.01$ is assumed on all subdomains, $l \in \mathcal{I}$.

Figure 8a shows the relative error norms over time for a simulation of 1000 time steps of size $\tau = 1 \cdot 10^{-3}$. The LDD-TP–R parameters were set to $L_{w,l} = 0.01$, $L_{nw,l} = 0.004$ and $\lambda^{lk}_{w} = 1$ as well

TABLE 3 TP–R coupling on a five-domain with inner subdomain: assumed coefficient functions and manufactured solutions

	Richards	**two-phase**
Data	Ω_1, Ω_5	Ω_2-Ω_4
$k_{w,l}(s)$	s^2	s^3
$k_{nw,l}(s)$	$(1-s)^2$	$(1-s)^3$
$S_l(p_c)$	$\begin{cases} \frac{1}{(1+p_c)^{1/2}} & p_c \geq 0 \\ 1 & p_c < 0 \end{cases}$	$\begin{cases} \frac{1}{(1+p_c)^{1/3}} & p_c \geq 0 \\ 1 & p_c < 0 \end{cases}$
$p^e_{w,l}(x,y,t)$	$-7-\left(1+t^2\right)\left(1+x^2+y^2\right)$	$-7-\left(1+t^2\right)\left(1+x^2\right)$
$p^e_{nw,l}(x,y,t)$	-	$\left(-3-t\left(1+y+x^2\right)-t^2\right)y^2$

TABLE 4 TP–R coupling on five-domain with inner subdomain: assumed soil parameters for case with same intrinsic permeabilities and porosities

	Richards		**Two-phase**			
Parameter	Ω_1, Ω_5		Ω_3		Ω_2, Ω_4	
Φ_l	0.2		0.2		0.2	
$k_{i,l}$	0.01		0.01		0.01	
h_l	0.071		0.070		0.071	
α	w	nw	w	nw	w	nw
μ_α[kg/(ms)]	1	-	1	$\frac{1}{50}$	1	$\frac{1}{50}$
ρ_α $\left[\text{kgm}^{-3}\right]$	997	-	997	1.225	997	1.225

as $\lambda^{lk}_{nw} = 0.25$ for all $l \in \mathcal{I}$ and $k \in \mathcal{I}_k$. The error of the nonwetting phase of the inner subdomain Ω_3, which is the worst of all phases and subdomains stays consistently below $5 \cdot 10^{-3}$. The nonwetting phases of Ω_2 and Ω_4 do not surpass $1 \cdot 10^{-3}$ and all wetting phases stay below $2 \cdot 10^{-4}$. The nonwetting phase on the inner subdomain shows a degradation in accuracy whereas the other phase errors are in line with the two-domain examples.

Figure 8b shows the subsequent errors for the time step t_{1000}. The stopping criterion was $\epsilon_s = 1 \cdot 10^{-6}$ and was reached after 202 iterations. The first time step required 106 iterations.

5.2.2 | Including gravity

The behavior of the solver when gravity is taken into account is shown in Figure 9b. To stabilize the solver, it was necessary to adjust the LDD-TP–R parameters to $L_{\alpha,l} = 0.5$ and $\lambda^{lk}_\alpha = 4$ for all phases $\alpha = w, nw$, $l \in \mathcal{I}$ and $k \in \mathcal{I}_l$. A tilting behavior in the subsequent error curves can be seen. This leads to plateaus in the curves and consequently, 370 iterations were required for time step $t_{1000} = 1.0$ to achieve the stopping criterion with $\epsilon_s = 5 \cdot 10^{-6}$. During the calculation for the first time step, 193 iterations were required. Albeit the solver exhibiting more struggle, the overall approximation quality, despite oscillating a bit seems unaffected as Figure 9a shows. The error of the nonwetting phase of the inner subdomain remains under $5 \cdot 10^{-3}$ for all times, and all other errors are lower. The tilting behavior and occurrence of plateaus was observed for all examples featuring the inclusion of gravity and is most probably due to the inherent instability of standard finite element methods for advection-dominated regimes.

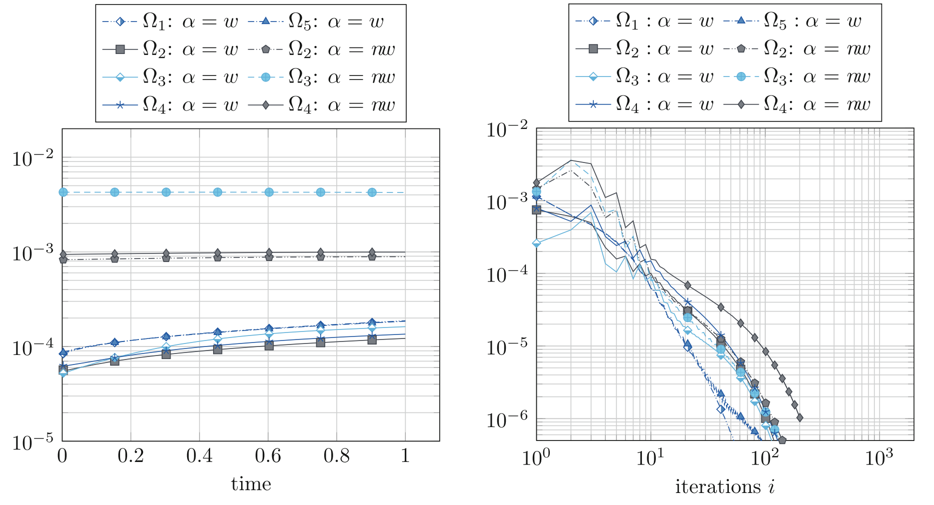

(a) Relative error norms $\|p^{e,n}_{\alpha,l} - p^{h,n}_{\alpha,l}\|_2 / \|p^{e,n}_{\alpha,l}\|_2$ over time t for all occurring (α, l).

(b) Subsequent errors $\|p^{h,i}_{\alpha,l} - p^{h,i-1}_{\alpha,l}\|_2$ over iteration i at time step $n = 1000$, $t_n = 1.0$.

FIGURE 8 TP–R coupling on five-domain substructuring with inner subdomain: Relative error norms (a) and subsequent errors at a fixed time step (b) for a simulation over 1000 time steps with same intrinsic permeabilities and porosities, *excluding gravity* and parameters $h \approx 0.070$–0.071, $\tau = 1 \cdot 10^{-3}$, $L_{w,l} = 0.01$, $L_{nw,l} = 0.004$ and $\lambda_w^{lk} = 1$, $\lambda_{nw}^{lk} = 0.25$, $l \in \mathcal{I}$, $k \in \mathcal{I}_l$

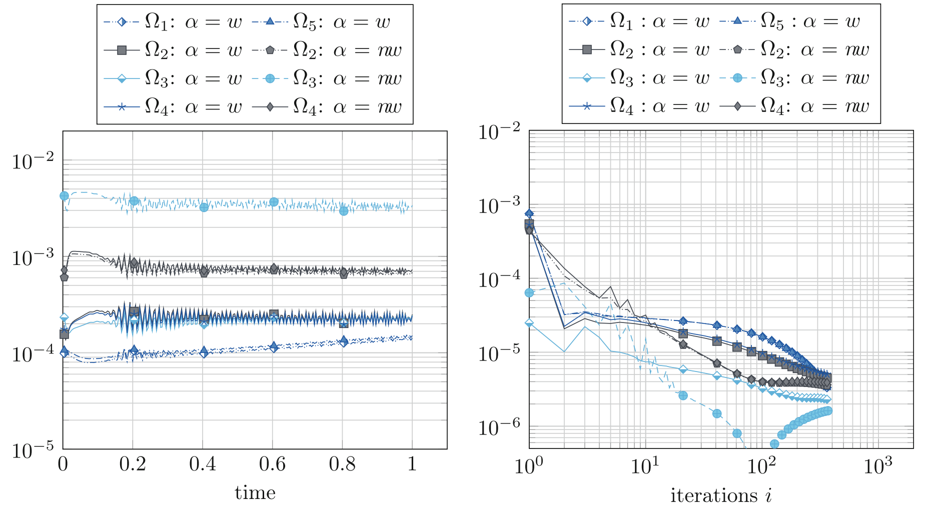

(a) Relative error norms $\|p^{e,n}_{\alpha,l} - p^{h,n}_{\alpha,l}\|_2 / \|p^{e,n}_{\alpha,l}\|_2$ over time t for all occurring (α, l).

(b) Subsequent errors $\|p^{h,i}_{\alpha,l} - p^{h,i-1}_{\alpha,l}\|_2$ over iteration i at time step $n = 1000$, $t_n = 1.0$.

FIGURE 9 TP–R coupling on five-domain substructuring with inner subdomain: Relative error norms (a) and subsequent errors at a fixed time step (b) for a simulation over 1000 time steps with same intrinsic permeabilities and porosities, *including gravity* and parameters $h \approx 0.070$–0.071, $\tau = 1 \cdot 10^{-3}$, $L_{\alpha,l} = 0.5$, and $\lambda_\alpha^{lk} = 4$, for all appearing $\alpha \in \{w, nw\}$ and $l \in \mathcal{I}$, $k \in \mathcal{I}_l$

6 | CONCLUSIONS

In this article, we proposed a new domain decomposition approach for hybrid two-phase flow systems. For new coupling conditions between domains with different two-phase flow models we developed an approach combining an *L*-type linearization of the nonlinearities with a generalized nonoverlapping alternating Schwarz method, the LDD-TP–R solver. This formulation unifies the work of both, [1] and

[2] on homogeneous two-phase models and allows for the treatment of complex modeling situations involving very heterogeneous soil parameters. The LDD-TP–R solver has been analyzed rigorously on the time-discrete level. Numerical experiments for two- and multidomain settings confirm the theoretical findings. In particular, they show the possible gain of computing time when using the hybrid model instead of employing an expensive full two-phase model on the entire domain.

As the LDD-TP–R solver linearizes and decouples the substructured problem, it can either be used as a pure domain decomposition method, as a basis for effective parallel computation, or in a model-adaptive domain decomposition setting, in which an envisioned model change (two-phase/Richards) dictate the substructuring. Future work will be directed to design such an algorithm that might also include an adaptive choice of models based on our error analysis. We envisage that our approach is not only effective for the basic two-phase flow models encountered here but can be also extended to more complex model hierarchies for multiphase flow and/or multicomponent transport.

ACKNOWLEDGMENTS

The authors thank the German Research Foundation (DFG) for funding this work (Project Number 327154368–SFB-1313). In parts, this work was supported by E.ON Stipendienfonds (Project Number T0087/30890/17) which funded a research stay at the University of Bergen (UIB) for which the authors are grateful. Open Access funding enabled and organized by Projekt DEAL.

DATA AVAILABILITY STATEMENT

Data available on request from the authors

ORCID

David Seus https://orcid.org/0000-0002-6460-0561

REFERENCES

[1] D. Seus, K. Mitra, I. S. Pop, F. A. Radu, and C. Rohde, *A linear domain decomposition method for partially saturated flow in porous media*, Comput. Methods Appl. Mech. Eng. 333 (2018), 331–355. https://doi.org/10.1016/j.cma.2018.01.029.

[2] D. Seus, F. A. Radu, and C. Rohde, "A linear domain decomposition method for two-phase flow in porous media," *Numerical mathematics and advanced applications ENUMATH 2017*, Lecture Notes in Computational Science and Engineering, F. A. Radu, K. Kumar, I. Berre, J. M. Nordbotten, and I. S. Pop (eds.), Springer International Publishing, Switzerland, 2019, pp. 603–614. https://doi.org/10.1007/978-3-319-96415-7_55.

[3] P.-L. Lions, "On the Schwarz alternating method," *Proceedings of the 1st international symposium on domain decomposition methods for partial differential equations*, R. Glowinski, G. H. Golub, G. A. Meurant, and J. Periaux (eds.), SIAM, Philadelphia, 1988, pp. 1–42.

[4] I. S. Pop, F. A. Radu, and P. Knabner, *Mixed finite elements for the Richards' equation: Linearization procedure*, J. Comput. Appl. Math. 168 (2004), no. 1–2, 365–373. https://doi.org/10.1016/j.cam.2003.04.008.

[5] F. List and F. A. Radu, *A study on iterative methods for solving Richards' equation*, Comput. Geosci. 20 (2016), no. 2, 341–353. https://doi.org/10.1007/s10596-016-9566-3.

[6] M. S. Agranovich, *Sobolev spaces, their generalizations and elliptic problems in smooth and Lipschitz domains*, Springer Monographs in Mathematics, Springer International Publishing, Switzerland, 2015. https://doi.org/10.1007/978-3-319-14648-5.

[7] A. Quarteroni, A. Valli, Domain decomposition methods for partial differential equations, repr. Edition, *Numerical mathematics and scientific computation*, Clarendon Press, Oxford, UK, Oxford, UK, 2005.

[8] V. Dolean, P. Jolivet, and F. Nataf, "An introduction to domain decomposition methods," *Algorithms, theory, and parallel implementation*, Society for Industrial and Applied Mathematics (SIAM), Philadelphia, PA, 2015. https://doi.org/10.1137/1.9781611974065.ch1.

[9] D. Bennequin, M. J. Gander, L. Gouarin, and L. Halpern, *Optimized Schwarz waveform relaxation for advection reaction diffusion equations in two dimensions*, Numer. Math. 134 (2016), 513–567.

[10] J. O. Skogestad, E. Keilegavlen, and J. M. Nordbotten, *Domain decomposition strategies for nonlinear flow problems in porous media*, J. Comput. Phys. 234 (2013), 439–451. https://doi.org/10.1016/j.jcp.2012.10.001.

[11] H. Berninger, R. Kornhuber, and O. Sander, *A multidomain discretization of the Richards equation in layered soil*, Comput. Geosci. 19 (2015), no. 1, 213–232. https://doi.org/10.1007/s10596-014-9461-8.

[12] D. A. Di Pietro, E. Flauraud, M. Vohralík, and S. Yousef, *A posteriori error estimates, stopping criteria, and adaptivity for multiphase compositional darcy flows in porous media*, J. Comput. Phys. 276 (2014), 163–187.

[13] E. Ahmed, S. A. Hassan, C. Japhet, M. Kern, and M. Vohralík, *A posteriori error estimates and stopping criteria for space-time domain decomposition for two-phase flow between different rock types*, SMAI J. Comput. Math. 5 (2019), 195–227. https://doi.org/10.5802/smai-jcm.47.

[14] M. Kuraz, P. Mayer, and P. Pech, *Solving the nonlinear richards equation model with adaptive domain decomposition*, J. Comput. Appl. Math. 270 (2014), 2–11. https://doi.org/10.1016/j.cam.2014.03.010.

[15] M. Gander, S. Lunowa, C. Rohde, Non-overlapping Schwarz waveform-relaxation for nonlinear advection-diffusion equations, Preprint, http://www.uhasselt.be/Documents/CMAT/Preprints/2021/UP2103.pdf (2021).

[16] S. B. Lunowa, I. S. Pop, and B. Koren, *Linearized domain decomposition methods for two-phase porous media flow models involving dynamic capillarity and hysteresis*, Comput. Methods Appl. Mech. Eng. 372 (2020), 113364. https://doi.org/10.1016/j.cma.2020.113364.

[17] E. Ahmed, C. Japhet, and M. Kern, *Space–time domain decomposition for two-phase flow between different rock types*, Comput. Methods Appl. Mech. Eng. 371 (2020), 113294.

[18] M. A. Borregales Reverón, K. Kumar, J. M. Nordbotten, and F. A. Radu, *Iterative solvers for biot model under small and large deformations*, Comput. Geosci. 25 (2021), no. 2, 687–699. https://doi.org/10.1007/s10596-020-09983-0.

[19] D. Illiano, I. S. Pop, and F. A. Radu, *Iterative schemes for surfactant transport in porous media*, Comput. Geosci. 25 (2021), no. 2, 805–822. https://doi.org/10.1007/s10596-020-09949-2.

[20] M. A. Celia, E. T. Bouloutas, and R. L. Zarba, *A general mass-conservative numerical solution for the unsaturated flow equation*, Water Resour. Res. 26 (1990), no. 7, 1483–1496. https://doi.org/10.1029/90WR00196.

[21] K. Mitra and I. Pop, *A modified L-scheme to solve nonlinear diffusion problems*, Comput. Math. Appl. 77 (2019), no. 6, 1722–1738. https://doi.org/10.1016/j.camwa.2018.09.042.

[22] L. Qin and X. Xu, *On a parallel Robin-type nonoverlapping domain decomposition method*, SIAM J. Numer. Anal. 44 (2006), no. 6, 2539–2558. https://doi.org/10.1137/05063790X.

[23] Q. LiZhen, S. ZhongCi, and X. XueJun, *On the convergence rate of a parallel nonoverlapping domain decomposition method*, Sci China Ser A Math 51 (2008), no. 8, 1461–1478. https://doi.org/10.1007/s11425-008-0103-2.

[24] L. Qin and X. Xu, *Optimized Schwarz methods with Robin transmission conditions for parabolic problems*, SIAM J. Sci. Comput. 31 (2008), no. 1, 608–623. https://doi.org/10.1137/070682149.

[25] X. Na and X. Xu, *An optimal Robin-Robin domain decomposition method for stokes equations*, Appl. Numer. Math. 171 (2022), 426–441. https://doi.org/10.1016/j.apnum.2021.09.015.

[26] R. Helmig, *Multiphase flow and transport processes in the subsurface: A contribution to the modeling of hydrosystems*, Springer, Berlin, 1997 http://swbplus.bsz-bw.de/bsz061703095err.htm.

[27] J. Bear, *Hydraulics of groundwater*, Dover Books on Engineering, Dover Publications, 2007.

[28] L. A. Richards, *Capillary conduction of liquids through porous mediums*, Physics 1 (1931), no. 5, 318–333. https://doi.org/10.1063/1.1745010.

[29] L. F. Richardson, *Weather prediction by numerical process*, Camebridge University Press, Cambridge, 2007 https://archive.org/stream/weatherpredictio00richrich#page/n0/mode/2up/search/Darcy.

[30] M. Henry, D. Hilhorst, and R. Eymard, *Singular limit of a two-phase flow problem in porous medium as the air viscosity tends to zero*, Discrete Contin. Dyn. Syst. Ser. S 5 (2012), no. 1, 93–113. https://doi.org/10.3934/dcdss.2012.5.93.

[31] C. Cancès and M. Pierre, *An existence result for multidimensional immiscible two-phase flows with discontinuous capillary pressure field*, SIAM J. Math. Anal. 44 (2012), no. 2, 966–992. https://doi.org/10.1137/11082943X.

[32] H. Berninger, *Domain decomposition methods for elliptic problems with jumping nonlinearities and application to the Richards equation*, Ph.D. thesis, FB Mathematik und Informatik, Freie Universität Berlin, 2009. http://www.diss.fu-berlin.de/diss/receive/FUDISS_thesis_000000008972

[33] F. Brezzi and M. Fortin, *Mixed and hybrid finite element methods*, Springer Series in Computational Mathematics, Vol 15, Springer, Cham, 1991.

[34] W. McLean, *Strongly systems and boundary integral equations*, Cambridge University Press, Cambridge, 2000, pp. 357.

[35] P. L. Lions, "On the Schwarz alternating method III: A variant for nonoverlapping subdomains," *Third international symposium on domain decomposition methods for partial differential equations*, Society for Industrial and Applied Mathematics, T. F. Chan, R. Glowinski, J. Périaux, and O. B. Widlund (eds.), Philadelphia, 1990, pp. 202–223.

[36] D. Seus, LDD schemes for two-phase flow systems, Reihe Mathematik, Dr. Hut Verlag, 2021. https://www.dr.hut-verlag.de/978-3-8439-4874-6.html

[37] F. A. Radu, K. Kumar, J. M. Nordbotten, and I. S. Pop, *A robust, mass conservative scheme for two-phase flow in porous media including Hölder continuous nonlinearities*, IMA J. Numer. Anal. 38 (2017), 884–920. https://doi.org/10.1093/imanum/drx032.

[38] M. S. Alnæs, J. Blechta, J. Hake, A. Johansson, B. Kehlet, A. Logg, C. Richardson, J. Ring, M. E. Rognes, and G. N. Wells, *The FEniCS project version 1.5*, Arch. Numer. Software 3 (2015), no. 100, 9-23. https://doi.org/10.11588/ans.2015.100.20553.

[39] A. Logg, G. N. Wells, and J. Hake, *DOLFIN: A C++/python finite element library*, Springer, Cham, 2012 Ch. 10.

[40] D. Seus, https://gitlab.com/davidseus/ldd-for-two-phase-flow-systems (2021).

How to cite this article: D. Seus, F. A. Radu, and C. Rohde, *Towards hybrid two-phase modelling using linear domain decomposition*, Numer. Methods Partial Differ. Eq. **39** (2023), 622–656. https://doi.org/10.1002/num.22906